Journal of South American Earth Sciences 111 (2021) 103487

Contents lists available at ScienceDirect

Journal of South American Earth Sciences

journal homepage: www.elsevier.com/locate/jsames

Tectono-stratigraphic evolution of the northeastern sector of the Ñirihuau basin, North Patagonian Andes, Argentina: Insights from sedimentology and geochronology data of the Ñirihuau Formation

Camila Santonja [a,b,*], Florencia Bechis [a,c], Julieta Suriano [a,d], Juan I. Falco [a,c], Alfonso Encinas [e], Ezequiel R. Olaizola [a,c], Victor A. Valencia [f], Vanesa D. Litvak [a,g], Victor A. Ramos [a,g]

[a] Consejo Nacional de Investigaciones Científicas y Técnicas (CONICET), Argentina
[b] Universidad de Buenos Aires, Instituto de Geociencias Básicas, Aplicadas y Ambientales de Buenos Aires (IGEBA), UBA-CONICET, Ciudad Universitaria, Pabellón II, Intendente Güiraldes 2160 (C1428EHA), Buenos Aires, Argentina
[c] Universidad Nacional de Río Negro, Instituto de Investigaciones en Diversidad Cultural y Procesos de Cambio (IIDyPCa), UNRN-CONICET, San Carlos de Bariloche, Argentina
[d] Instituto Argentino de Nivología, Glaciología y Ciencias Ambientales (IANIGLA), CONICET, CCT Mendoza, Argentina
[e] Universidad de Concepción, Departamento Ciencias de la Tierra, Facultad de Ciencias Químicas, Chile
[f] Washington State University, School of the Environment, USA
[g] Universidad de Buenos Aires, Instituto de Investigaciones Andinas "Don Pablo Groeber" (IDEAN), UBA-CONICET, Ciudad Universitaria, Buenos Aires, Argentina

ARTICLE INFO

Keywords:
Cenozoic
Andean evolution
Patagonia
Miocene
Rift basin
Foreland basin
Continental sedimentary environments

ABSTRACT

An approximately 3500 m thick stratigraphic section was detailed surveyed in order to study the tectono-sedimentary evolution of the Ñirihuau Formation along the Arroyo Las Bayas, in the northern sector of the Ñirihuau basin, North Patagonian Andes. A total amount of 29 lithofacies were recognized and used to define facies, grouped into six facies associations (FA) that reflect different paleoenvironments: FA1 (Gray to brownish conglomerates), FA2 (Conglomerates and sandstones), FA3 (Tabular mudstones), FA4 (Brownish sandstones and conglomerates with large scale foresets), FA5 (White tuffaceous sandstones) and FA6 (Sandstones and conglomerates with mudstones). The lower section of the unit was interpreted as deposited in a medium to distal alluvial fan or an axial fluvial system developed in the most distal zone of an alluvial fan (FA1 and FA2). The middle section of the unit is characterized by a Gilbert-type delta developed between two lacustrine sequences (FA3 and FA4). In the upper section of the unit, higher energy deposits corresponding to fluvial systems are registered (FA5 and FA6). Deposits from synchronic volcanic events are recorded along the stratigraphic section. Also, a provenance analysis was carried out by using sedimentary petrography and U–Pb zircon geochronology data. The main identified sediment source corresponds to the contemporaneous Miocene volcanic arc. A secondary detrital provenance from older Cenozoic volcanic rocks of the El Maitén Volcanic Belt was also identified, as well as minor contributions from pre-Cenozoic igneous and metamorphic units. U–Pb geochronological data constrain deposition of the middle and upper sections of the Ñirihuau Formation in the Arroyo Las Bayas section to the middle to late Miocene, between 15 and 11.4 Ma (Langhian to Tortonian). Also, a possible middle Miocene age was discussed for the lower section. An integrated tectono-stratigraphic model was finally proposed, with contrasting extensional and synorogenic tectonic stages registered in the lower and upper sections of the Ñirihuau Formation, respectively.

1. Introduction

The Cenozoic sedimentary evolution of the Ñirihuau basin in northwest Patagonia took place during a period of contrasting tectonic regimes registered in a long segment of the Southern Central Andes from Oligocene to Miocene times, probably related to variations in the subduction dynamics (Jordan et al., 2001; Charrier et al., 2007; Bechis et al., 2014a; Horton, 2018; Butler et al., 2020).

The Ñirihuau basin was developed in an intra-to retroarc position and was located between 41° and 43° SL at the eastern side of the North

* Corresponding author. Consejo Nacional de Investigaciones Científicas y Técnicas (CONICET), Argentina.
E-mail addresses: cs.santonja@gmail.com, camilasantonja@gl.fcen.uba.ar (C. Santonja).

https://doi.org/10.1016/j.jsames.2021.103487
Received 1 December 2020; Received in revised form 17 July 2021; Accepted 20 July 2021
Available online 24 July 2021

Patagonian Andes (Fig. 1) (Cazau, 1972, 1980; Cazau et al.,1989, 2005). There is no generalized consensus about its origin. The first tectonic interpretations considered it as a typical foreland basin associated with the Andean uplift at these latitudes, with subsidence associated with the tectonic load (Ramos and Cortés, 1984; Giacosa et al., 2001; Giacosa and Heredia, 1999). Dalla Salda and Franzese (1987) and Spalletti and Dalla Salda (1996) assigned a transtensional origin, interpreting it as a pull-apart basin. These authors indicated that the reactivation of basement structures as strike-slip faults would have generated the opening and closing of several sedimentary basins behind the magmatic arc during Oligocene and Miocene times.

Most recent studies agree that the basin opening was associated to an

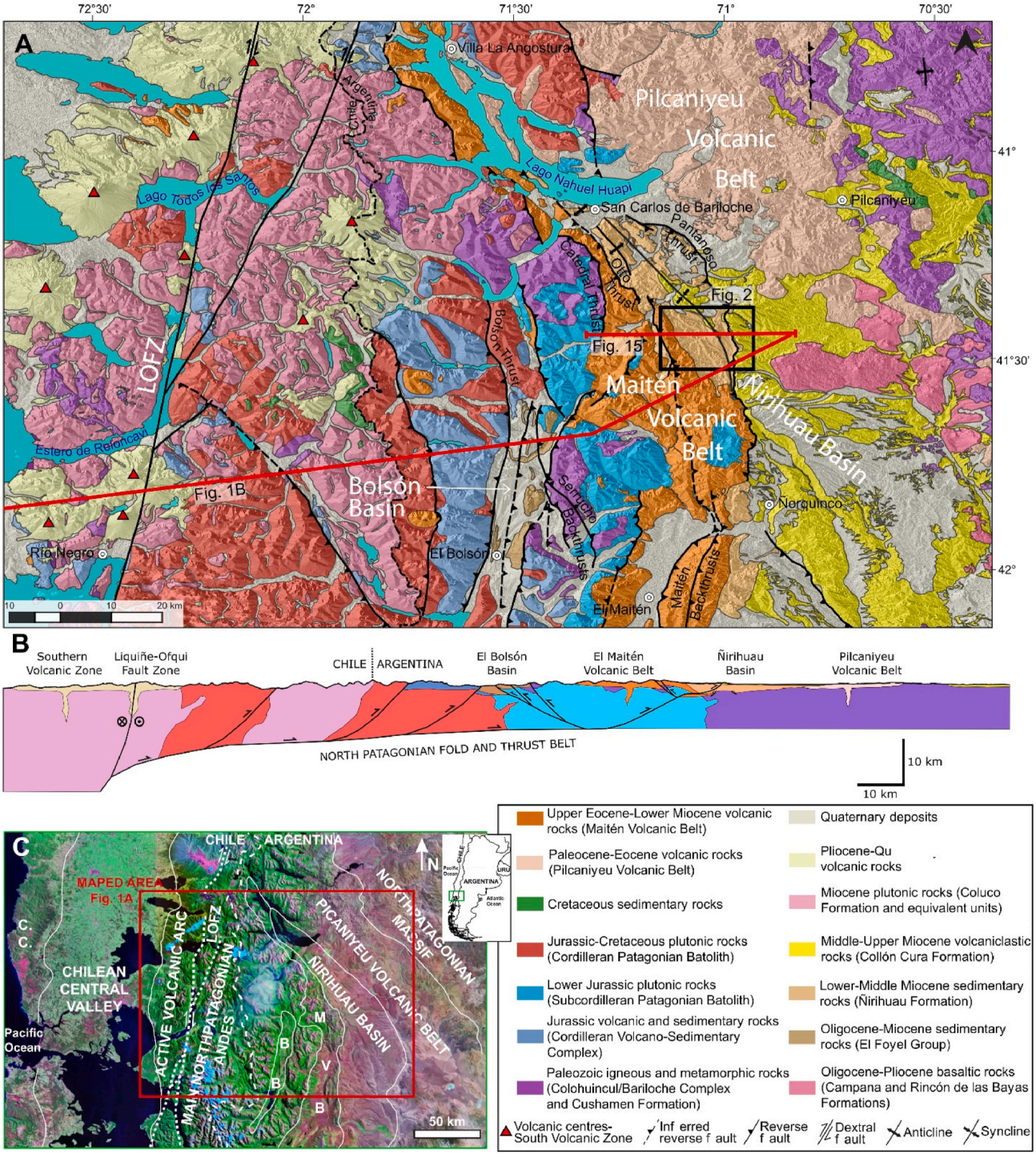

Fig. 1. A) Regional geologic map showing the geologic units and the main structures of the area (after González Bonorino, 1944; González et al., 2000; Giacosa et al., 2001; SERNAGEOMIN, 2003; Escosteguy et al., 2013; Bechis et al., 2014a; Tobal et al., 2015). The black box indicates the study area location (Fig. 2). B) Schematic regional cross-section, showing the main structural configuration of the North Patagonian fold and thrust belt and the current location of the Ñirihuau and El Bolsón basins (after Giacosa and Heredia, 2004a, Bechis et al., 2014a; Orts et al., 2015; Tobal et al., 2015). C) Landsat™ mosaic-based map showing the main regional morphostructural units (modified from Bechis et al., 2014a).LOFZ: Liquiñe-Ofqui Fault Zone, CC: Coastal Cordillera, BB: El Bolsón Basin, MVB: El Maitén Volcanic Belt.

extensional stage, which lasted until the late Oligocene or early Miocene, followed by a compressive regime from the early or middle Miocene to the Pliocene (Mancini and Serna, 1989; Bechis, 2004; Bechis and Cristallini, 2006; Bechis et al., 2014b; Orts et al., 2015). The precise dating of this proposed tectonic switching in the Ñirihuau basin remains poorly understood and is still under discussion. Paredes et al. (2009) interpreted that the compressional deformation in the north sector of the basin began during the latest stages of deposition of the Ñirihuau Formation, based on structural observations. Orts et al. (2012) suggested that the foreland basin progressed from 18 Ma, based on interpreted progressive unconformities in marine strata that crop out in the main North Patagonian Andes. Bilmes et al. (2013) proposed that a contractional episode occurred at ca. 16.1–14.86 Ma, in response to an eastward migration of the Andean fold and thrust belt, that led to the development of the Gastre basin in the foreland. Based on U–Pb ages, Ramos et al. (2015) proposed a contractional episode that migrated eastward from ~19 to 15 Ma, producing the Gastre broken foreland, and then retracted to the eastern North Patagonian Andes, where out of sequence thrust cannibalized the wedge top zone in El Maitén volcanic belt at ~13.5–11.3 Ma. On the other hand, Bechis et al. (2015) interpreted that the tectonic switching in the eastern sector of the North Patagonian Andes took place later, sometime between 16 and 13 Ma (middle Miocene). Also, Butler et al. (2020) mentioned that middle Miocene growth strata in the Ñirihuau Formation suggest that shortening had commenced by ~13-12 Ma.

The filling of the eastern sector of the Ñirihuau basin consists of a thick sequence of Oligocene to lower Miocene volcanic rocks (Ventana Formation) and Miocene volcaniclastic, clastic and carbonatic rocks deposited mainly in continental environments (Ñirihuau and Collón Curá Formations). K–Ar ages had initially assigned the Ñirihuau Formation to the early Miocene (22-16 Ma; Cazau et al., 1989), but recent U–Pb data from the southeastern sector of the basin suggest an early to middle Miocene age for the unit (22-12 Ma; Ramos et al., 2015; Butler et al., 2020).Therefore, a detailed analysis of the Ñirihuau Formation is key for the understanding of the basin evolution and could shed light on the tectonic setting and the timing of the main changes registered in this sector of the North Patagonian Andes. In this contribution we present a detailed sedimentological analysis and new geochronological data of the Ñirihuau Formation exposures along the upper course of the Arroyo Las Bayas, located in the northern sector of the Ñirihuau basin. With these data, the depositional environments, provenance areas, depositional ages, and evolution of the unit were interpreted. In addition, together with previous local and regional structural data, we intend to establish a tectono-stratigraphic evolution for this sector of the basin. The studied stratigraphic section is one of the most extensive, continuous, and less known of the Ñirihuau Basin. Thus the presented results constitute an important contribution for the understanding of the tectono-stratigraphic evolution of the Ñirihuau basin.

2. Geological setting

The North Patagonian Andes stratigraphic record was divided by Giacosa et al. (2005) into three major lithological associations: the pre-Mesozoic basement; the Mesozoic plutonic, volcanic, and sedimentary rocks; and the Cenozoic plutonic, volcanic and sedimentary rocks.

The basement consists of high to medium grade igneous-metamorphic rocks, product of a Late Paleozoic metamorphism and deformation of Precambrian to Paleozoic rocks during the Gondwanides orogeny (Ramos, 1999). In the Andean region, these rocks are assigned to the Colohuincul Complex (Turner, 1965; Dalla Salda et al., 1991; García Sansegundo et al., 2009) or to the Bariloche Complex, according to a recent proposal (Oriolo et al., 2019) (Fig. 1). Towards the east, in the foreland region, these rocks are assigned to the Cushamen Formation (Fig. 1) (Volkheimer, 1964; González Díaz and Nullo, 1980).

The Early Jurassic Argentine-Chilean Andes were characterized by a convergent regime associated with extension that led to the formation of depocenters with volcano-sedimentary filling (Ramos, 1988). In this region, these rocks were included in the Cordilleran Volcano-Sedimentary Complex (Fig. 1) (Giacosa et al., 2001). Synchronic to the development of these depocenters, the plutonic rocks that constitute the Subcordilleran Patagonian Batholith were intruded along the eastern sector of the North Patagonian Andes (Fig. 1) (Gordon and Ort, 1993; Pankhurst et al., 2006). Later, the Cordilleran Patagonian Batholith, with Middle Jurassic to Cretaceous ages, was emplaced mainly along the Andean axis (Fig. 1) (Giacosa et al., 2001; Castro et al., 2011; and references therein). Based on the calc-alkaline character of these rocks, this Andean segment was interpreted as an active margin with an intermittent magmatic activity since the Early Jurassic (Castro et al., 2011).

A change in the tectonic regime is registered by the late Early Cretaceous, going from extensional to compressive (Somoza and Zaffarana, 2008; Gianni et al., 2018). In the North Patagonian Andes, this tectonic switching is evidenced by angular unconformities separating Jurassic from Lower Cretaceous rocks (Tobal et al., 2012; Orts et al., 2012; Echaurren et al., 2016).

The Paleogene period in the eastern side of the North Patagonian Andes was characterized by the eruption of important volumes of volcanic material of the Andesitic Series, which were divided into two subparallel belts according to their ages, composition and facies distribution (Feruglio, 1941, 1947, 1949; Rapela et al., 1988). The Pilcaniyeu Volcanic Belt (Extra-Andean Series) is located to the east of the Ñirihuau basin (Fig. 1), with ages from the late Paleocene to the middle Eocene (~57-42 Ma). It was developed along a NW strip (Fig. 1) that presents initially silicic volcanism followed by andesites in its northern sector, while towards the southeast it is characterized by a bimodal volcanism that includes basalts and mostly acidic ignimbrites facies (Rapela et al., 1988, Aragón and Mazzoni, 1997; Aragón et al., 2011, 2018; Iannelli et al., 2017, 2020). The late Eocene to early Miocene (~37-19 Ma) El Maitén Volcanic Belt (Andean Series) is located to the west, in the sub-Andean region (Fig. 1). It conforms a NNW belt with dominance of andesitic and dacitic volcanic rocks with minor amount of rhyolites, basalts and pyroclastic rocks, while the sequences located in the northern sector of this volcanic belt exhibit intercalation of volcaniclastic sediments and contain marine beds constrained within the early Miocene (González Bonorino and González Bonorino, 1978; Rapela et al., 1988; Bechis et al., 2014a, 2014b; Benedini et al., 2017; Fernández Paz et al., 2018, 2019, 2020). The volcanic rocks from the Pilcaniyeu and El Maitén belts were grouped in the Huitrera and Ventana Formations, respectively (Ravazzoli and Sesana, 1977; González Bonorino and González Bonorino, 1978).

During the Oligocene, coincident with an important plate reorganization (Pardo Casas and Molnar, 1987; Somoza, 1998), a number of basins were developed between 33° and 45° S, with a late Oligocene to Miocene infill constituted by volcaniclastic continental deposits and marine intercalations (Jordan et al., 2001). Two distinct Cenozoic basins or sub-basins have been identified near the study area, which could have been originally connected but are currently separated by basement blocks uplifted during the Andean compression and by volcanic outcrops of the El Maitén Volcanic Belt (Fig. 1) (Giacosa and Heredia, 1999). The westernmost depocenters were included in the El Bolsón basin (Giacosa and Heredia, 1999, 2004a, 2004b, 2004a), where Oligocene to Miocene marine and continental sequences included in the El Foyel Group are exposed along an intermontane valley (Feruglio, 1941; Diez and Zubia, 1981; Ramos, 1982; Barreda et al., 2003; Asensio et al., 2005, 2010; Bechis et al., 2014a). The eastern depocenters are part of the Ñirihuau basin, which is located between 41° and 43°30' at the eastern side of the North Patagonian Andes (Fig. 1) (Cazau, 1972, 1980; Cazau et al., 1989, 2005). This basin has an elongated shape, with a N to NW direction that could be linked to a control of the previous basement structures (Bechis and Cristallini, 2005). It is also markedly asymmetric, with the principal depocenters located at its western border (Giacosa et al., 2005). Its infill is characterized by volcanic and sedimentary rocks included in the

Nahuel Huapi Group, of Oligo-Miocene age, which is constituted by the Ventana, Ñirihuau and Collón Curá Formations (Cazau et al., 1989, 2005, 2005; González Bonorino and González Bonorino, 1978; Bechis et al., 2014a, 2014b, 2015, 2014b; Ramos et al., 2015; Butler et al., 2020). It has been suggested that the El Bolson and Ñirihuau basins would have been connected in the early Miocene (23-16 Ma), during a marine transgression related to an extensional tectonic stage that took place during the Oligocene to early Miocene, before the main contractional phase that gave place to the uplift of the North Patagonian Andes (Bechis et al., 2014a; Fernández Paz et al., 2019, 2020). The eastward advance of the orogenic front produced the final segmentation of the original larger basin, separating these two depositional areas (Paredes et al., 2009).

During the Miocene the principal episode of North Patagonian Andes uplift took place, and the volcanic and sedimentary sequences of the Nahuel Huapi Group were deformed, together with the uplift of basement blocks (Ramos and Ghiglione, 2008; Folguera et al., 2011). This compressive deformation gave rise to a fold and thrust belt, with a predominantly thick-skinned structural style (Ramos and Cortés, 1984; Giacosa and Heredia, 2004a, 2004b, 2004b; Giacosa et al., 2005). In the eastern subandean sector, the upper infill of the Ñirihuau basin presents growth strata and angular unconformities that register the frontal propagation of the deformation during the Miocene (Bechis, 2004; Giacosa et al., 2005; Bechis and Cristallini, 2005, 2006, 2006; Bechis et al., 2015; Ramos et al., 2011, 2015, 2015; Orts et al., 2015).

Miocene granitoids constitute great part of the western sector of the cordillera, while they extend towards the east in more restricted outcrops at around 41°S, where they were grouped in the Coluco Formation (Fig. 1) (González Díaz, 1979). The Pliocene to Recent volcanic arc is also restricted to the western area, where the active volcanoes of the Southern Volcanic Zone are located (Fig. 1) (Stern, 2004; Lara et al., 2001). During the Pliocene, the frontal sector of the fold and thrust belt became inactive, and the tectonic activity moved towards the Chilean sector, where the deformation has been accommodated by the dextral to transpressional Liquñe Ofqui Fault System (Fig. 1) (Lavenu and Cembrano, 1999; Folguera and Ramos, 2002; Thomson, 2002; Adriasola et al., 2005; Rosenau et al., 2006).

3. The Ñirihuau Formation

The Ñirihuau Formation was identified by Roth (1922), and formally defined by González Bonorino (1973). The unit was described southeast of San Carlos de Bariloche city (Fig. 1), and it was considered equivalent to the Ñorquinco Formation, which was originally defined in the southeastern sector of the Ñirihuau basin (Cazau, 1972; Giacosa et al., 2001; Bechis et al., 2014a).

The Ñirihuau Formation constitutes part of the clastic and volcaniclastic infill of the Ñirihuau basin (Fig. 2). Its thickness varies along the basin, with a maximum of 3500 m of well-stratified sediments registered east of the Cordón de Las Bayas (Mancini and Serna, 1989; Bechis, 2004). The studied stratigraphic section along the Arroyo Las Bayas was chosen because of the high quality of its exposures, being one of the most extensive and continuous outcrops of the Ñirihuau Formation. This unit consists of clastic and volcaniclastic deposits with subordinate carbonatic rocks deposited predominantly in the Miocene (Cazau, 1972, 1980, 1980; González Bonorino and González Bonorino, 1978; Spalletti, 1981; Cazau et al., 1989; Mancini and Serna, 1989; Bechis, 2004; Giacosa et al., 2005; Paredes et al., 2009; Ramos et al., 2015; Bechis et al., 2015; Butler et al., 2020). As the provenance of the material that constitutes the Ñirihuau Formation is mostly volcanic (Spalletti and Matheos, 1987), previous studies considered it as the same effusive series that gave place to the Ventana Formation (Ljunger, 1931; Cazau et al., 2005). However, it differs from the underlying unit due to its predominantly sedimentary character.

The contact relationship between the Ventana and the Ñirihuau Formations from the Nahuel Huapi Group has had different interpretations. Some authors have interpreted this contact as concordant (Ljungner, 1931; Feruglio, 1941), as an angular unconformity (Groeber, 1954; Dessanti, 1972; Cazau, 1972) or variable according to the position in the basin (González Bonorino and González Bonorino, 1978). A concordant to transitional passage between these units was observed in the eastern side of Cordón de Las Bayas, at the western sector of our study area. Regarding the relationship between the Ñirihuau Formation and the overlying Collón Curá Formation, an angular unconformity was described in the Cerro David (David Formation, *sensu* González Bonorino, and Gonzalez González Bonorino and González Bonorino, 1978), while a transitional passage is determined by an increase in the pyroclastic intercalations in areas away from the Andean thrust front (Cazau et al., 1989). In our studied area, a tectonic contact between the Ñirihuahu and Collón Curá formations along the Pantanoso thrust was recognized (Fig. 2) (Rabassa, 1978; Bechis, 2004; Giacosa and Heredia, 2004a; Giacosa et al., 2005).

The Ñirihuau Formation was interpreted as deposited in alluvial, lacustrine, deltaic and fluvial environments (Cazau, 1972, 1980; Spalletti, 1981; Cazau et al., 1989; Mancini and Serna, 1989; Giacosa et al., 2005; Paredes et al., 2009; Ramos et al., 2011). These environments were also recognized in our study area (section 5). The unit registers a markedly decrease in the volcanic activity in comparison with the Ventana Formation; although the pyroclastic sedimentation was predominant in some levels indicating that the volcanism was still active during the Ñirihuau Formation deposition (González Bonorino and González Bonorino, 1978; Cazau et al., 1989; Paredes et al., 2009).

Although the Ñirihuau Formation is predominantly continental, a sea connection was proposed during the deposition of its middle member. This was based on sedimentary structures that suggest tidal influence (Spalletti, 1981, 1983, 1983; Asensio et al., 2004), on the appearance of marine microfossils (dinoflagellates and acritarchs) found in exploration wells samples (Cazau et al., 1989), as well as on the discovery of marine mollusks (González Bonorino and González Bonorino, 1878; Ramos, 1982). Nevertheless, the predominance of a freshwater environment is evidenced by skeletons of osseous fish registered in Cerro David, Arroyo Las Bayas and Arroyo Pantanoso (Bocchino, 1964; Aragón and Romero, 1984; Pascual et al., 1984; Cione and Baez, 2007), crustacea preserved on the lower member of the Ñirihuau Formation (Aguirre Urreta, 1992), and ostracods from *candona* genus found in different pelitic levels from the deep lacustrine facies (Cazau et al., 1989).

Abundant fossil flora remains were identified in deposits of the Ñirihuau Formation, including dicotyledons from the *Nothofagus* flora, that would have developed under a temperate to warm-temperate and humid climate, and dryer conditions towards the top of the unit (Aragón and Romero, 1984; Passalia and Bechis, 2012; Falaschi et al., 2012; Caviglia and Zamaloa, 2014; Passalia et al., 2019; Caviglia, 2018).

4. Methodology

An approximately 3,500m thick stratigraphic section of the Ñirihuau Formation along the Arroyo Las Bayas was detailly surveyed (Figs. 2 and 3), with a vertical scale of 1:2000 (Fig. 4). Partial stratigraphic sections (sections A-F) were surveyed in the field and later compiled in a general integrated section, in order to avoid structural disturbances related to minor folding (Figs. 3 and 4). Three informal units were defined in this work for the Ñirihuau Formation based on their predominant lithology, in order to achieve a more detailed mapping of the structures and to control the continuity of the stratigraphic sections (Figs. 2 and 3). Correlations between the partial stratigraphic sections were also based on regional volcaniclastic marker beds (Fig. 2; i. e. green tuff). The Ñirihuau Formation was characterized according to its lithology, sedimentary structures, and bed geometries. Facies and facies associations were determined in order to interpret the depositional paleoenvironment after Miall (1978, 1996) (Table 1). A few carbonatic layers were described according to the Dunham classification (Dunham, 1962)

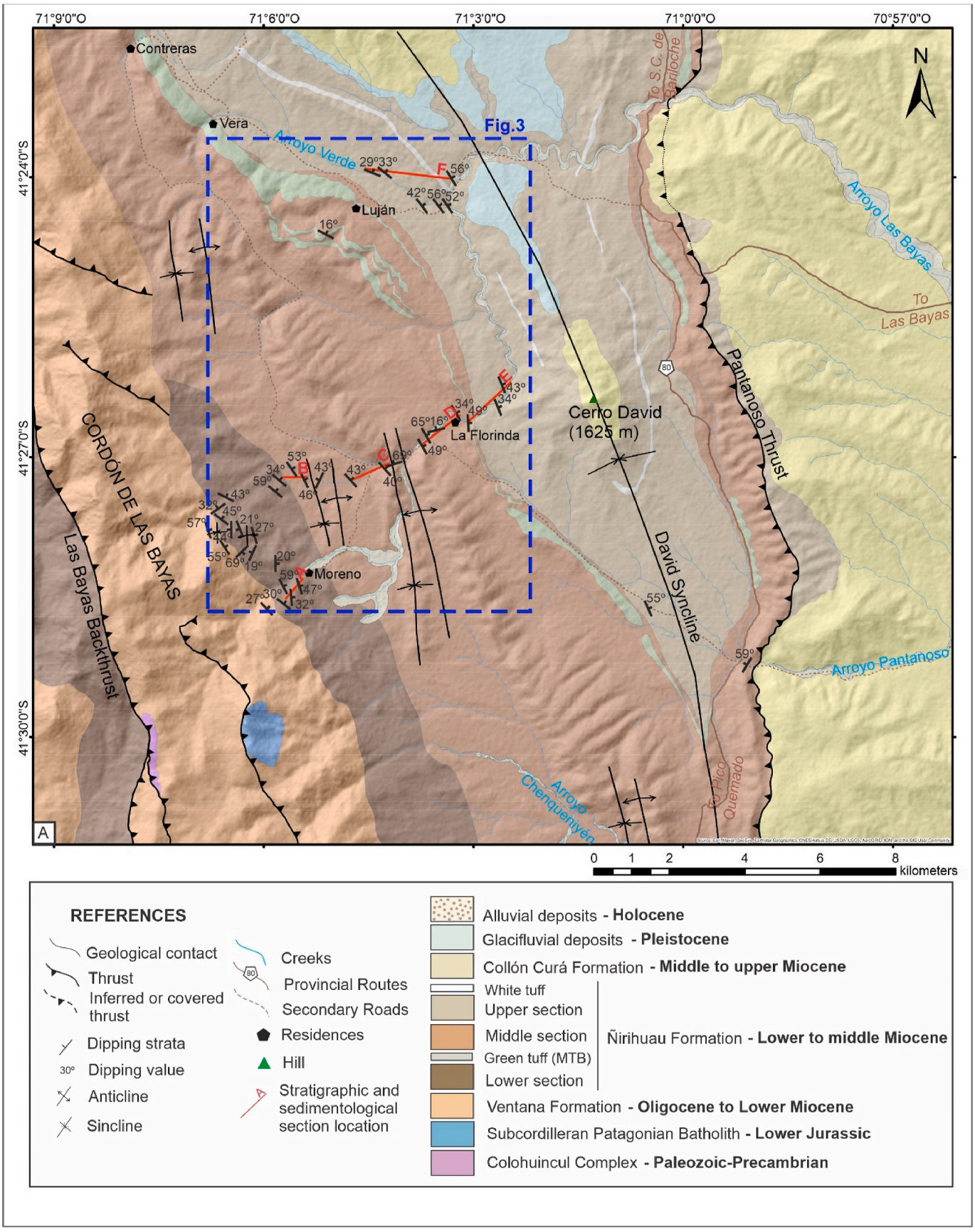

Fig. 2. Geologic map of the study area (see Fig. 1A for location) and location of the stratigraphic sections along the Arroyo Las Bayas. MTB: "Miembro Tobas y Brechas" defined by González Bonorino and González Bonorino (1978).

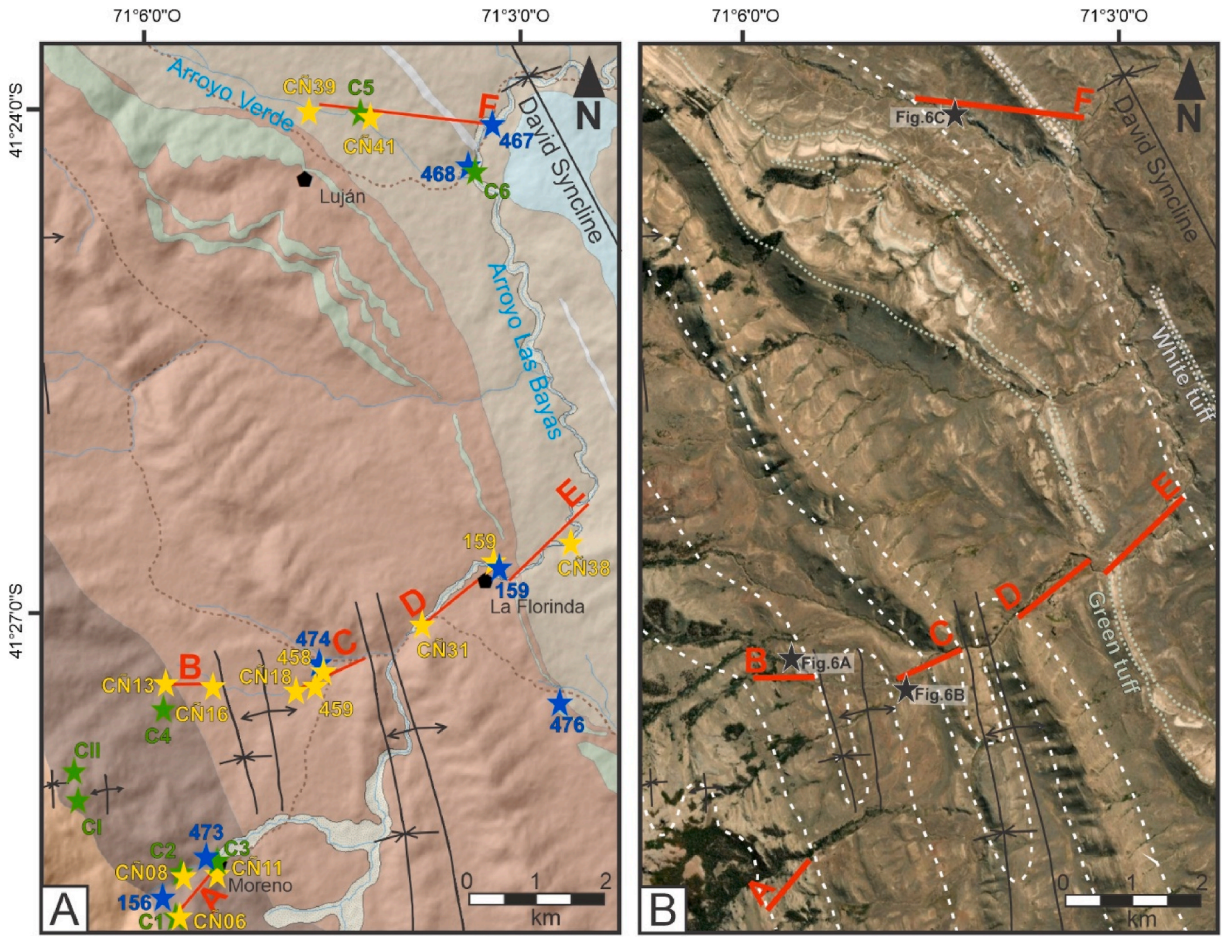

Fig. 3. A) Geologic map with the location of the partial sections surveyed for the Ñirihuau Formation along the Arroyo Las Bayas (A to F partial sections indicated in red). The location of the conglomerate clast countings (green stars), the sandstones samples for petrography analysis (yellow stars) and the sedimentary rocks and tuffs samples for LA-ICP MS U–Pb analysis in zircons (blue stars) is also indicated in the map. See Fig. 2 for location and references. B) Satellite image with the location of the partial sections (A to F, indicated in red). The strata used to connect the partial stratigraphic sections are indicated by white dashed lines. Green tuff ("Miembro Tobas y Brechas") and white tuff deposits were also used as marker beds in the field. Black stars show the location of the structural data illustrated on the photographs of Fig. 6.

modified by Wright (1992). In the present work, the term volcaniclastic is used after White and Houghton (2006). These authors defined that primary volcaniclastic rocks and deposits are accumulations of particles that were mobilized directly by explosive or effusive volcanism, also including deposits of uncertain origin, like "resedimentated syn-eruptive volcaniclastic" (after McPhie et al., 1993). Those deposits that are not directly related to eruptions but with volcanic heritage are considered "epiclastic", which are formed by the weathering of primary volcanic and volcaniclastic rocks (Fisher, 1961).

During the field activities, clast counting in conglomerates was done according to the methodology proposed by Cavazza (1989). Also, sandstone samples for petrographic analyses were taken along the stratigraphic section. Additionally, a total of seven samples along the studied stratigraphic section were collected and LA-ICP-MS U–Pb analyses in zircons were conducted, both in igneous zircons from tuffs and in detrital zircons from sedimentary rocks. This geochronological data was used to constrain the depositional age of the Ñirihuau Formation in the studied section, and the age of the probable sediment sources. With all this information, a provenance analysis was carried out.

Finally, with the information obtained from the different performed analyses and taking into consideration the regional geological setting, an interpretation for the tectono-stratigraphic evolution of the area was made.

4.1. Sandstone petrography

Thirteen representative sandstone samples were collected and analyzed under the microscope, and eighteen modal components were identified. The modal composition quantification performed on the samples was done according to the Gazzi-Dickinson methodology (Ingersoll et al., 1984 and references therein), counting between 200 and 300 grains per sample. From the results of the modal thin section analysis, sandstones were classified according to Folk et al. (1970). Finally, these values were plotted in the provenance ternary Qm-F-Lt and Qt-F-L diagrams proposed by Dickinson et al. (1983) to discriminate the tectonic source areas.

Percentage and type of matrix, cement and porosity of sandstones samples were also distinguished, analyzing both the textural characterization and modal composition. Mean and maximum granulometry of the grains were determined according to the Udden-Wentworth scale (Wentworth, 1922). The type of grain contact was defined after Taylor (1950). The selection was estimated by visual comparisons (Harrel, 1984) as well as the sphericity and roundness (Powers, 1953; Pettijohn et al., 1973). All thin sections were impregnated with blue epoxy resin before thin-section preparation for the recognition of optical porosity, which was classified according to Boggs (2009).

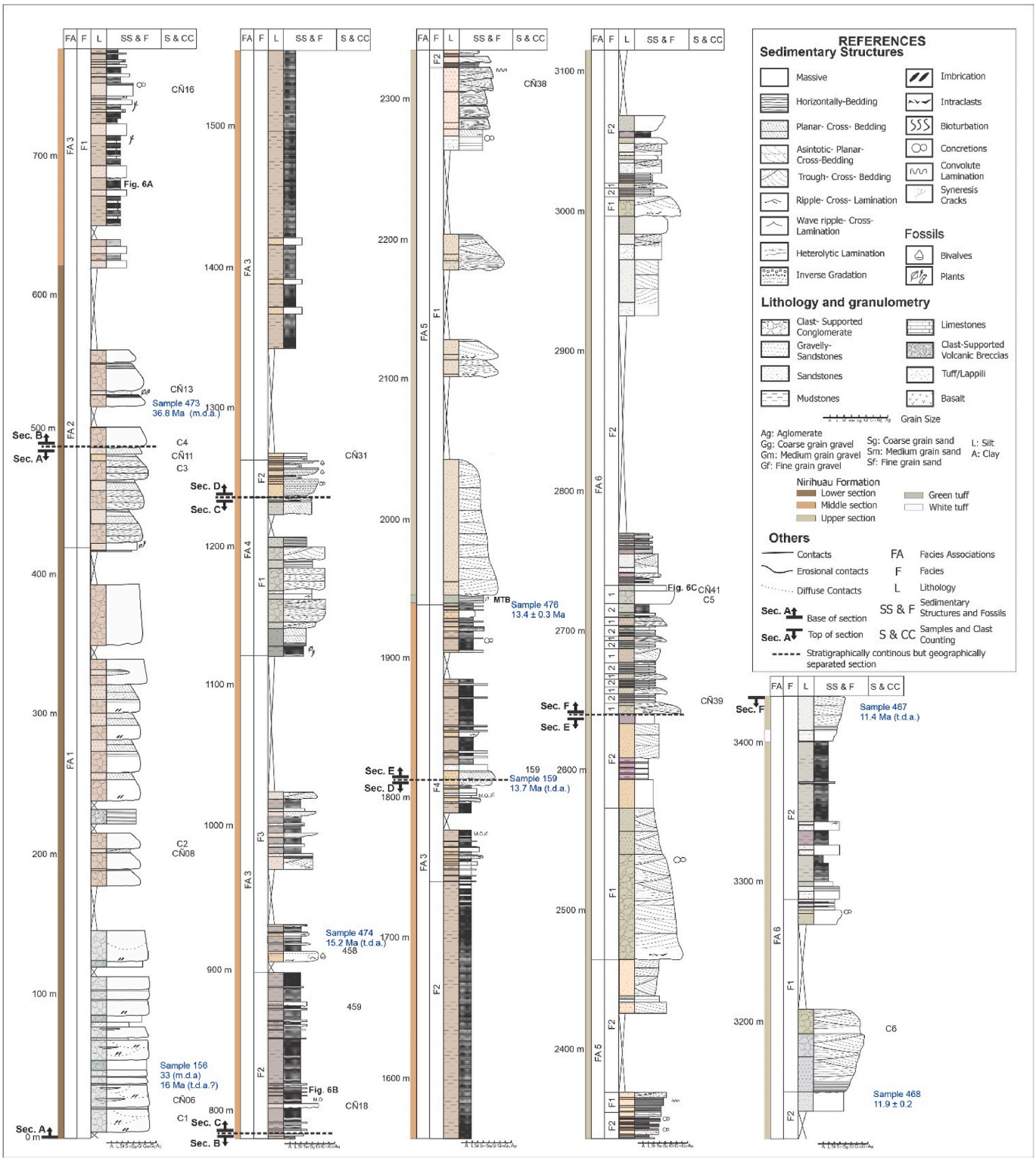

Fig. 4. Composite stratigraphic section of the Ñirihuau Formation along the Arroyo Las Bayas. See figures 2 and 3 for location of the surveyed partial sections (A to F). MTB: "Miembro Tobas y Brechas" sensu González Bonorino and González Bonorino (1978); M.O.: organic matter; m.d.a.: maximum depositional age; t.d.a.: true depositional age.

4.2. U–Pb geochronology

Five sedimentary rocks samples (156, 473, 474, 159, 467) and two tuff samples (476, 468) were collected from the studied stratigraphic section of the Ñirihuau Formation along the Arroyo Las Bayas (Figs. 3 and 4). All seven samples were analyzed for zircon U–Pb LA-ICP-MS geochronology.

Heavy mineral concentrates of the <350 μm fraction were separated using traditional techniques at ZirChron LLC and LA.TE. ANDES. Zircons from the non-magnetic fraction were mounted in epoxy and slightly ground and polished to expose the surface and keep as much material as possible for laser ablation analyses. Most of the LA-ICP-MS U–Pb

Table 1
Lithofacies identified along the stratigraphic section studied of the Ñirihuau Formation (modified from Miall, 1996).

Code	Lithofacies
Gcm	Clast- supported massive conglomerate
Gch	Clast-supported horizontally stratified conglomerate
Gcp	Clast- supported planar-cross-bedded conglomerate
Gct	Clast- supported trough-cross-bedded conglomerate
Gci	Clast- supported imbricated conglomerate
Gc_i	Clast- supported conglomerate with Intraclasts
Sm	Massive sandstone
Sh	Horizontally bedded sandstone
Sl	Low-angle cross-bedded sandstone
Sp	Planar- cross-bedded sandstone
St	Trough-cross-bedded sandstone
Sr	Ripple cross-laminated sandstone
Srw	Wave ripple cross-laminated sandstone
Sht	Heterolithic sandstone
Sb	Bioturbated sandstone
Si	Sandstone with intraclasts
Fm	Massive mudstone
Fl	Laminated mudstone
Fb	Bioturbated mudstone
MSm	Massive limestone
GRh	Horizontally bedded limestone
GRr	Ripple-cross-laminated limestone
GRrw	Wave-ripple-cross-laminated limestone
GRht	Heterolytic limestone
GRi	Limestone with intraclasts
Tm	Massive tuff
Tl	Laminated tuff
Tgi	Inverse-Graded tuff
V	Volcanic rocks and volcanic breccias

analyses were conducted at Washington State University using a New Wave Nd:YAG UV 213-nm laser coupled to a ThermoFinnigan Element 2 single collector, double-focusing, magnetic sector ICP-MS following operating procedures and parameters from Chang et al. (2006). Additional analyses for sample 156 were carried out at LA.TE. ANDES, with a LA-ICP-MS combination instrumental: RESOlution ablation laser 193 nm manufactured by Australian Scientific Instrument and triple quadrupole ICP-MS 8900 model manufactured by Agilent Technologies. For all samples, U–Pb ages were calculated using Isoplot (Ludwig, 2003). The final ages include systematic and analytical errors of around 2% (2*s*).

5. Facies analysis and depositional paleoenvironments

Six facies associations (FA) were identified in the Ñirihuau Formation stratigraphic section surveyed along the Arroyo Las Bayas (Table 2). They were used to define the sedimentary paleoenvironments in this unit, and their evolution through time. According to their predominant lithology, FA1 and FA2 were included in the lower section; FA3 and FA4 in the middle section; and finally, FA5 and FA6 correspond to the upper section of the Ñirihuau Formation (Fig. 4).

5.1. FA1: Gray to brownish conglomerates

Description: This facies association is constituted by both laterally and vertically amalgamated lenticular bodies of 1,5 to 3 m thick, with erosive bases (Fig. 5A). Clast-supported massive conglomerates (Gcm) are dominant with a minor proportion of clast-supported imbricated conglomerates (Gci) and clast-supported horizontally stratified conglomerates (Gch). The clasts are subrounded and have a maximum size (Xmax) of 51 cm. The coarser-grain conglomerates had a mean clast size (X½) of 18 cm (Fig. 5A) and are more abundant than the finer-grain conglomerates, with X½ of 5 cm. Towards the top of these bodies, very low proportions of sandstones with horizontal (Sh), planar cross-bedded (Sp) and trough cross-bedded (St) stratification are interbedded. These thinner grain size intercalations become more abundant towards the top of the facies association (Fig. 4). There are also a few volcaniclastic intercalations of green volcanic breccias (Vb) and, in lower proportion, white tuffs and lapilli-tuffs (Tm) (Fig. 3).

Interpretation: The clast-supported conglomerates in amalgamated lenticular bodies, with decreasing energy sedimentary structures (Gcm, Gci, Gch, Sp, Sh) and a few sandy intercalations, are interpreted as a braided fluvial system constituted by multi-storey gravel channels (Miall, 1996), dominated by longitudinal bars (Bridge and Tye, 2000; Bridge, 2006). As it will be further analyzed in the Discussion section, these channels would correspond to the middle zone of an alluvial fan (Miall, 1985; Einsele, 1992; Blair and McPherson, 1994a, 1994b, 1994b; Nichols, 2009). The volcanic processes were active during deposition of this facies association, represented by thin bodies of pyroclastic flows (volcanic breccias) and ash-fall deposits (massive tuffs and lapilli-tuffs (Tm)), interbedded among the conglomeratic deposits.

5.2. FA2: Conglomerates and sandstones

Description: This association is constituted by clast-supported planar cross-bedded conglomerates (Gcp), as well as planar cross-bedded and horizontally bedded sandstones (Sp and Sh). It constitutes a thickening upwards succession of both lateral and vertically amalgamated lenticular bodies that individually exhibit a thinning upwards tendency and erosional bases (Fig. 5B). They exhibit clasts up to 10 cm (Xmax), with a X½ of 5 cm. In this facies association, very well-preserved fossil flora remains were recognized (Passalia and Bechis, 2012). A thin basaltic level was also observed (40 cm) in the lowermost portion of this facies (near the 400 m of the stratigraphic section; Fig. 4).

Although this facies association has very similar characteristics to the previous one, it was differentiated due to the higher proportion of sandstones and to the smaller grain size of its conglomerates (Fig. 4).

Interpretation: The lenticular bodies with erosional bases and decreasing energy shown by the diminishing grain size and sedimentary structures (Gcp, Sp, Sh), are interpreted as a braided sandy-conglomeratic fluvial system dominated by transversal bars (Miall, 1996; Posamentier and Walker, 2006). These channels would have been deposited in a distal alluvial fan or in a braided fluvial system (Miall, 1985; Einsele, 1992; Blair and McPherson, 1994a, 1994b).

5.3. FA3: Tabular mudstones

Description: This unit exhibits great exposures of mudstones with a few interbedded sandstones, tuffs, and limestones (Fig. 4). It was subdivided into four different facies (Table 2).

The Facies 1 is constituted principally by massive and laminated mudstones and siltstones (Fm and Fl) that contain fossil flora remains. Intercalations of both fine and coarse-grained sandstones are observed. The fine-grained sandstones have either wave-ripple (Srw) or current-ripple (Sr) cross-lamination, while the coarse-grained sandstones have horizontal lamination. In a lower proportion, massive sandstones (Sm) are also observed. These deposits exhibit tabular geometries with, in general, a planar base and conform coarsening and thickening upwards successions from 2 to 7 m thick (Fig. 5C).

The most representative unit of this facies association is Facies 2, which is constituted mainly by mudstones with a few interbedded sandstones and volcaniclastic rocks (Fig. 4). The mudstones are observed as tabular bodies with planar bases. They show lamination (Fl) and bioturbation (Fb), and a high content of organic matter evidenced by the dark color of the deposit (Fig. 5D). The sandstone intercalations are tabular bodies with thicknesses ranging from 3 to 60 cm, and with erosive bases. They are either horizontally laminated or massive (Sh and Sm). There is also an exceptionally coarse sandstone lenticular body of great thickness (1.5 m) observed around the 800 m of the stratigraphic section surveyed (Fig. 4). Regarding the volcaniclastic deposits, well-lithified massive greenish gray tuffs levels were observed (Tm). These levels are about 60 cm thick and become more abundant towards the top

Table 2
Main characteristics of the facies associations recognized along the Ñirihuau Formation. The proportions of the different lithologies are indicated in approximate percentages in order to reflect their abundance.

Facies Associations	Characteristics	Facies (Lithofacies)	Interpretation	
			Facies	Facies Association
FA1:Gray to brownish conglomerates	Amalgamated lenticular bodies with volcanites interbedded and in lower proportions, sandstones. (G: 80%, V: 15%, S: 5%)	Gcm, Gci, Gch, Sh, Sp, Vb, Tm	Gravelly braided channels dominated by longitudinal bars -Middle alluvial fan	
FA2:Conglomerates and sandstones	Amalgamated lenticular conglomeratic bodies with lentiform sandy bodies interbedded. Coarsening and increasing thickness upwards tendency. (G: 70%, S: 30%)	Gcp, Sp, Sh	Sandy-gravelly braided channels dominated by transversal bars - Distal alluvial fan or axial fluvial system	
FA3:Tabular mudstones	Great thickness (up to 600 m) of tabular mudstones with variable thickness intercalations (from 2 to 60 cm) of tabular to lentiform sandstones, tuffs l and occasionally, limestones. (S:30%, F: 55%, V:10%, L: 5%)	Facies 1 Sr, Srw, Sh, Fm, Fl (S: 35%; F; 65%)	Near shore lake	Perennial lakes dominated by detrital clastic material with syndepositional volcanism.
		Facies 2 Sh, Sm, Fl, Fb, Tm (S:10%; F: 85%; V: 5%)	Deep lacustrine	
		Facies 3 Sh, Sr, Sp, Fl, Fm, GRh, GRr, GRrw, GRht, GRi, MSm, Tm, Tgi (S: 25%; F: 50%; V: 15%; L: 10%)	Intermediate to near shore lacustrine	
		Facies 4 Sht, Sh, Sr, St, Sp, Si, Sb, Fl, Tm (S: 45%; F: 25%; V: 30%)	Near shore zone with mouth bars	
FA4: Brownish sandstones and conglomerates with large scale foresets	Tabular to lenticular bodies of sandstones and conglomerates from 3 up to 10 m thickness, with subordinate thin levels of mudstones and volcaniclastic intercalations in low proportions. (G: 25%, S: 65%, F: 10%)	Facies 1 Gcp, Sh, Sr, Sp, Fl (G: 30%; S: 60%; F: 10%)	Deltaic front (Gilbert-type)	Deltaic System
		Facies 2 Gcp, Sp, Sr, Fl (G: 15%; S: 75%; F: 10%)	Delta plain	
FA5: White volcaniclastic sandstones	Mainly lentiforms sandstones and conglomerates bodies with tuff intercalations and few mudstones layers. (G:10%, S:65%, V:25%)	Facies 1 Gcp, Gct, Si, Sp, St, Sh, Sl, Sr, Tl (G: 20%; S: 60%; V: 20%)	Sandy channels	Volcaniclastic sandy braided fluvial system
		Facies 2 Sh, Sp, Sr, Fl, Fm, Tm, Tl (S: 65%; F: 5%; V: 30%)	Sandy-interchannel area	
AF6: Green sandstones and conglomerates with purple mudstones	Lenticular to tabular gravel and sandy bodies interbedded among mudstones bodies with high participation of volcaniclastic deposits. (G:20%; S: 30%; F: 35%; V: 15%)	Facies 1 Gcp, Gc_i, St, Sp, Sh, Sr, Si (G:40%; S:60%)	Sandy-gravelly channels	Anastomosed fluvial system
		Facies 2 Sp, St, Sr, Fl, Fm, Tl, Tm (F:70%; V:30%)	Muddy floodplain	

of the facies association. It is worth mentioning that normal faults were observed affecting these strata in several localities (Fig. 6A and B).

The Facies 3 is also constituted mainly by mudstones, but with higher proportions of sandstones and volcaniclastic deposits, as well as some isolated limestones (Fig. 5E). The mudstones are laminated (Fl) and massive (Fm). These deposits are observed as thin beds that exhibit a general coarsening upwards tendency. There are horizontally laminated, current-ripple cross-laminated and planar cross-bedded sandstones (Sh, Sr, Sp) in tabular bodies with erosional bases. The volcaniclastic deposits consist of white tuffs and lapilli-tuffs and are observed as thin intercalations (2–6 cm thick) among the mudstones. They become more abundant and thicker towards the top of the facies, and most of them exhibit inverse gradation (Tgi), although some levels are massive (Tm). The limestone bodies are tabular grainstones and calcimudstones. Grainstones show intraclasts (GRi), heterolytic-lamination (GRht), horizontal-lamination (GRh), current-ripple cross-lamination (GRr) and wave-ripple cross-lamination (GRrw), while calcimudstones are mainly massive (MSm) and have synsedimentary deformation (convoluted lamination and syneresis cracks). These limestone levels contain freshwater bivalve fossils (*Diplodon, Unionoida*).

Facies 4 is constituted mainly by sandstones, but it also includes volcaniclastic rocks and mudstones (Fig. 5F). Fine to medium grained sandstones are observed in lenticular bodies with heterolytic lamination (Sht), horizontal lamination (Sh) and current-ripple cross-lamination (Sr) in their base; and planar and trough cross-lamination (Sp and St) towards the top of the bodies. Some of them are highly bioturbated (Sb). Coarse-grained sandstones with lenticular geometry, erosional bases and diffuse planar cross-bedding are also observed. The volcaniclastic deposits are massive (Tm) and laminated (Tl) tuffs. In some sectors, they contain well-preserved fossil flora remains. Towards the top of the facies, the volcaniclastic deposits present higher thicknesses, reaching up to 3 m (Fig. 5F), and contain huge blocks (up to 20 cm). Finally, a few thin levels of laminated siltstones (Fl) with nodules were observed interbedded in the sandstones and tuffs.

Interpretation: This facies association is interpreted to reflect a lacustrine environment due to the predominance of fine grain size and laterally continuous deposits with thin laminations (Talbot and Allen, 1996).

Facies 1 is interpreted as a near shore lacustrine zone due to the granulometry, geometry, thicknesses and sedimentary structures of the deposits, that evidence a low energy environment with intercalated mudstones and sandstones in equal proportions (Reading, 1996; Paredes et al., 2009). These deposits exhibit sedimentary structures that are products of decantation processes (Fm), low regime fluid flows (Fl, Sh, Sr) and, in some cases, oscillatory flows (Srw) (Collinson and Thompson, 1989). The thin intercalations of laminated mudstones (Fl) with fine-grained sandstones are interpreted as the result of transport and deposition of fine-grained particles by a coherent plume of river water as it moves through the lake, generating hyperpycnal flows and eventually, overflows deposits, depending on the density of the inflow water relative to that of the lake water (Forel, 1892; Bates, 1953; Bhattacharya, 2006). Towards the facies top, a deepening of the lacustrine facies is inferred due to the decrease in the granulometry as well as the decrease in the thickness of the cycles.

The deepest paleoenvironment is registered in the Facies 2, evidenced by the great thicknesses of mudstones with presence of hyperpycnal and hyperpycnal flows deposits (Fl) (Lambert et al., 1976; Pharo and Carmack, 1979; Weirich, 1986). Its dark color indicates a low oxygenated system (Glenn and Kelts, 1991; Davidson, 1993). The sandstones intercalations (Sh, Sm) represent high energy flows deposits entering into the lake or coastal material re-sedimentation processes, which are relatively common in lakes (Talbot y Allen, 1996).

The Facies 3 is interpreted as deposited in an intermediate to near shore lacustrine zone due to the alternation of thin beds of sandstones and mudstones with planar base, which indicates coastline fluctuations (Paredes et al., 2009). This interpretation is reinforced by the presence

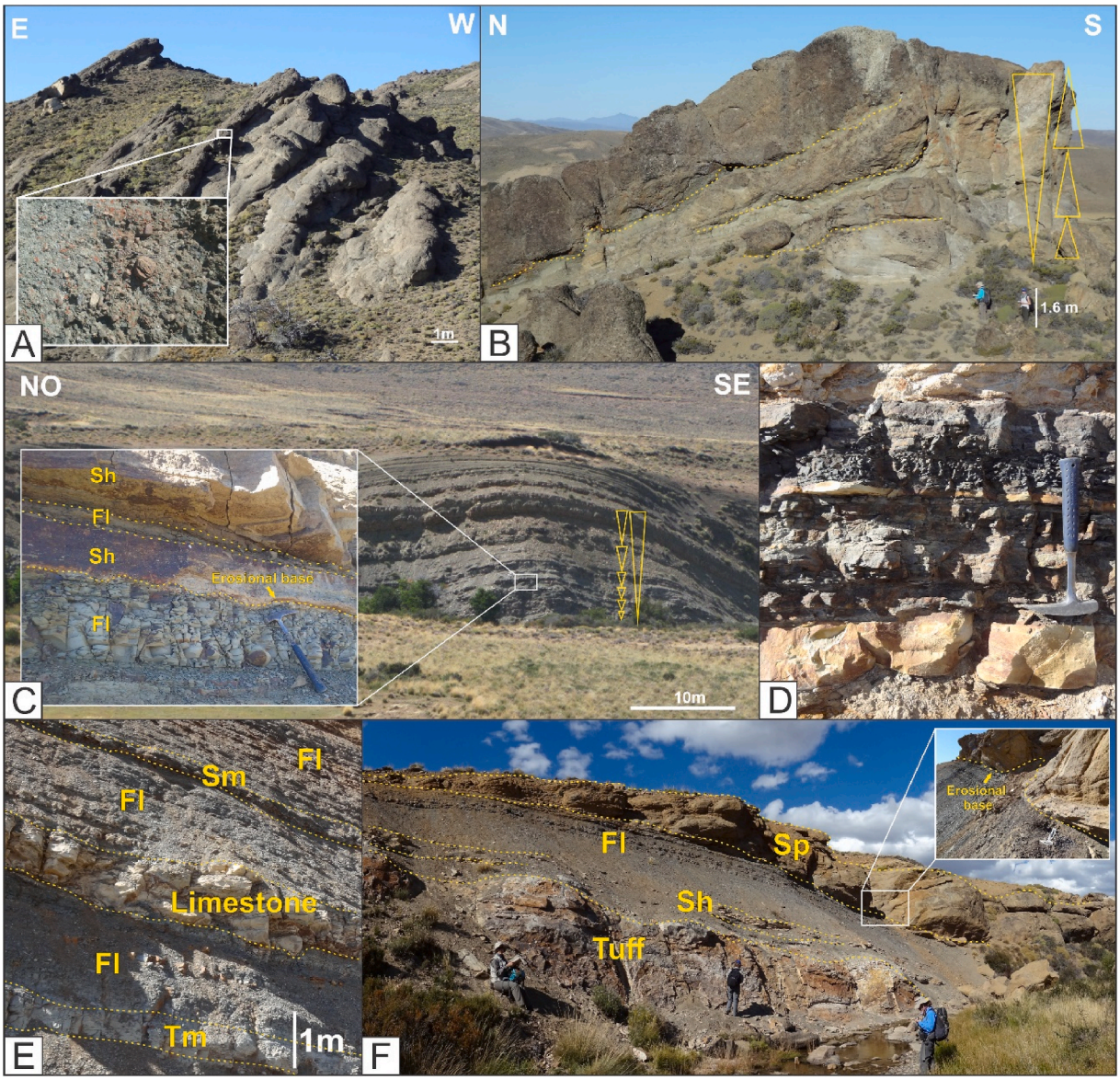

Fig. 5. Field photographs of sedimentary facies observed in the Ñirihuau Formation (Facies Associations 1, 2 and 3). A) Laterally and vertically amalgamated lenticular bodies from FA1. Inset showing a detail of clast-supported massive conglomerates with subrounded clasts. B) FA2 general aspect, showing coarsening upwards succession of bodies of increasing thicknesses with erosional bases, that individually show a thinning upwards tendency. C) Tabular bodies conforming coarsening and thickening upwards succession of laminated mudstones and siltstones with sandstones intercalations, described for the Facies 1 of FA3. D) Tabular mudstones with planar bases and a high content of organic matter, characteristic of the Facies 2 of FA3. E) Tuffs and limestones with synsedimentary deformation intercalated between laminated mudstones of the Facies 3 of FA3. F) Lenticular sandstone body on top of laminated mudstones from Facies 4 (FA3), showing planar cross-bedding and erosional bases. A 3 m thick volcanic deposit is also observed (tuff).

of low regime fluid flow structures (Fl, Fm, Sh, Sr) (Collinson and Thompson, 1989; Paredes et al., 2009) and carbonatic bodies (GRi, GRht, GRh, GRr, GRrw, MSm) containing bivalve fossils.

Finally, the lenticular sandstones bodies (Sh, Sp, St) with a few mudstones intercalations (Fl) observed in the Facies 4 are interpreted as mouth bars deposited in a near shore lacustrine zone related to a fluvial outlet zone (Reading and Collinson, 1996). It should be noticed that Facies 1 also corresponds to a near shore lacustrine area, but it represents a lateral zone, as there is no record of bar deposits in it.

According to the mentioned above, this facies association is interpreted to register somerization cycles of the lacustrine system, synchronic with a volcanic activity represented by the volcaniclastic intercalations registered mainly as ash-fall deposits (tuffs) and pyroclastic flows (lapilli-tuffs).

5.4. FA4: Brownish sandstones and conglomerates with large scale foresets

Description: Facies association 4 corresponds mainly to sandstones and conglomerates deposits, with subordinate levels of mudstones and a few volcaniclastic intercalations (Fig. 4). Two different facies were differentiated according to the scale and importance of their cycles (Table 2).

The Facies 1 shows a coarsening upwards tendency (Fig. 7A). Cycles are formed by sandstones and conglomerates, with lower proportions of mudstones and a scarce participation of volcaniclastic rocks. Fine-grained sandstones and thin mudstones intercalations (Fl) were observed at the basal portion of the facies, with tabular geometries and dominant planar bases. Internally the fine-grained sandstones are horizontally- (Sh) and current-ripple cross-laminated (Sr), and contain fossil

flora remains (Fig. 7B). These deposits are overlain by coarser sandstones showing large scale (up to 3 m), steeply dipping, planar cross-bedding (Sp) with concave-up geometries that have a marked angularity with the underlying beds (Fig. 7A and B). Finally, clast-supported conglomerates with tabular geometries are observed at the top of the cycles, exhibiting an internally fining upwards tendency (Xmax 3 cm and X½ 2 cm) and planar cross-bedded structures (Gcp).

The Facies 2 is predominantly sandy and presents subordinate proportions of conglomerates and mudstones. It is constituted by tabular bodies with erosional bases and an overall coarsening upwards tendency. Angular, sigmoidal and asymptotic towards the base planar cross-bedded (Sp), horizontally-laminated (Sh) and current-ripple cross-laminated sandstones (Sr) were observed (Fig. 7C). These levels contain bivalves' fossils in life position (Fig. 7D). Thin laminated mudstones (Fl) levels are interbedded with the thinner grained sandstones (Fig. 7C). In some cases, clast-supported conglomerate tabular bodies were observed on top of the sandstones, with a fining upwards tendency (Xmax 4 cm and X½ 3 mm) and planar cross-bedding (Gcp).

Interpretation: This facies association is interpreted as deposited in a fluvio-dominated deltaic system.

Facies 1 is interpreted as a Gilbert-type delta front, generated by the progradation of a river system into the lake. The lower finer deposits are interpreted as the bottomset, while the overlying coarser grained sandstone deposits showing steeply dipping cross-bedding, concave-up geometries and a marked angularity with the underlying beds are interpreted as foresets prograding against the bottomset (Nemec, 1990; Bornhold and Prior, 1990). These deltas are common in relatively deep lakes or fjords, related to high gradient margins (Nemec, 1990; Corner et al., 1990; Eilersten et al., 2011). The sandy and gravelly bodies with decreasing energy sedimentary structures (Gcp, Sp, Sh, Sr) and fining

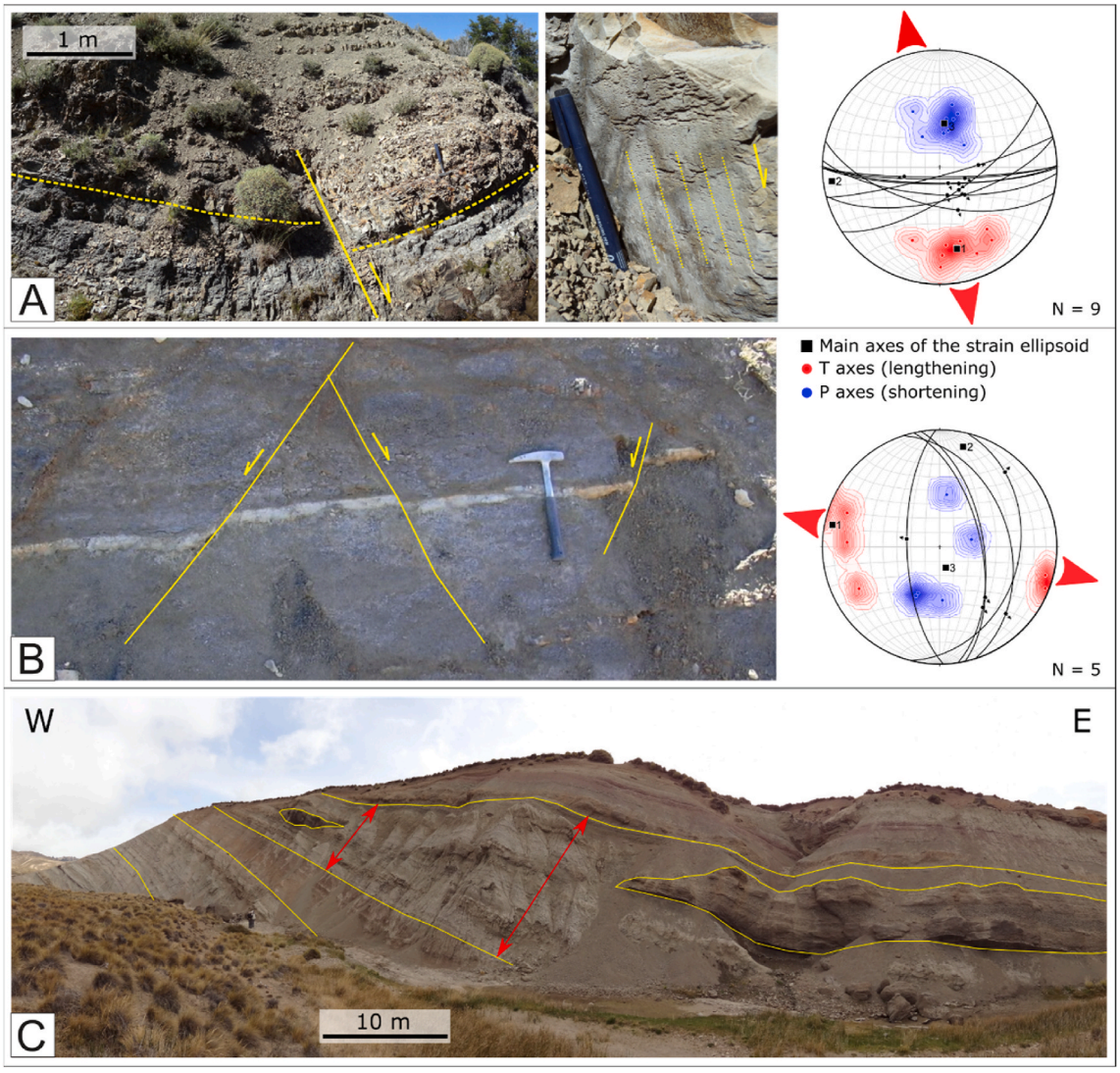

Fig. 6. A and B) Field photographs showing examples of normal faults affecting lacustrine strata in two localities of the Facies Association 3, in the lower middle section of the Ñirihuau Formation (see Figs. 3 and 4 for location). An example with a striated fault plane is also shown, where the high angle of the striae indicates a predominant dip slip of the fault. In the diagrams of the right side, major circles represent the lower-hemisphere projection of fault planes measured in each locality, with arrows showing the hanging-wall sense of movement. The distribution of principal incremental shortening and lengthening axes is shown for each location, and black squares represent the obtained axes of the strain ellipsoid (λ1, λ2 and λ3) for every group of faults. Big red arrows show the obtained extension direction for each locality. In both cases, analyzed fault slip data were rotated the amount necessary to return local bedding to horizontal, as they showed more coherent kinematics after the unfolding, suggesting that the faults are older than the folding related to shortening in the area (fold test; after Marret and Allmendinger, 1990). Kinematic diagrams obtained with the FaultKinWin® software (Allmendinger et al., 2012). C) Lateral thickness variations observed in the Facies Association 6 (upper section of the Ñirihuau Formation), which is interpreted as syntectonic growth strata. The observed thickening of the strata towards the east, where the axis of the David Syncline is located, could indicate that deposition was synchronic with the folding related to the frontal propagation of the fold and thrust belt.

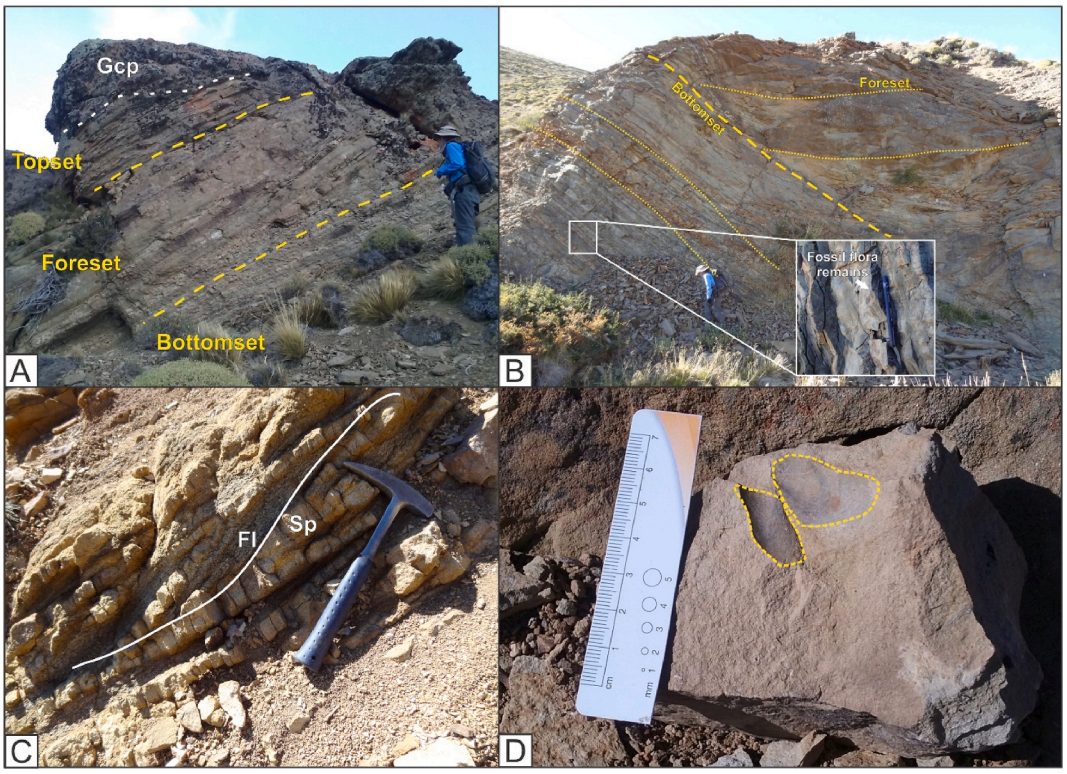

Fig. 7. Field photographs of Facies Association 4. A) Foresets with concave-up geometries and a coarsening upwards tendency of the Facies 1 can be observed. The bottomset, foreset and topset sections of the interpreted Gilbert-type delta are indicated. B) Cycles formed by tabular bodies of sandstones and conglomerates with lower proportions of mudstones of the Facies 1. Large scale, steeply dipping, cross-bedding with concave-up geometries showing a marked angularity with the underlying beds can be clearly appreciated in the photograph, which is interpreted as the progradation of foresets against the bottomset of a Gilbert-type delta. Inset showing a detail of the fossil flora remains, which were observed on the basal sector. C) Sigmoidal planar cross-bedded sandstones with interbedded thin laminated mudstones, observed in the Facies 2. D) Bivalves fossils observed on sandstones levels of the Facies 2.

upwards tendency were interpreted as the topset with channel deposits (Miall, 1996) with migration of gravelly transversal bars, that in occasions show mud drapes (Fl).

The Facies 2 overlies the previous one and it was interpreted as deposited in the delta plain. Inter-channel area is represented by flat-lying sandy bodies with unidirectional low regime fluid flow sedimentary structures (Bhattacharya, 2006; French, 2007), containing bivalves' fossils. The tabular sandy bodies with coarsening upwards tendency are interpreted as crevasse splays deposited in the floodplain (Sp, Sh, Sr) (Miall, 1996). The poorly preserved mudstones (Fl) are considered part of the delta plain inter-channel area (Harms et al., 1982). On the other hand, the coarser grained deposits (Gcp) were interpreted as channel deposits deposited in a delta plain prograding to a lacustrine system (Link et al., 1978).

Facies 2 overlies facies 1 in the stratigraphic section (Fig. 4), showing an overall coarsening upwards tendency. Therefore, the facies association 4 could have been deposited during the progradation of a fluvio-dominated deltaic system, where the deltaic front and the delta plain, with distributary channels, are preserved. The development of these kinds of forms are related to homopycnal river flows in steady waters (common in lacustrine environments) (Bhattacharya, 2006).

5.5. FA5: White tuffaceous sandstones

Description: Facies association 5 is mainly constituted by sandstones with high participation of volcaniclastic deposits and, in lower proportions, conglomerates and mudstones. It was divided into two different facies according to the granulometry of the deposits (Table 2).

The Facies 1 is mainly composed of sandstones and conglomerates with volcaniclastic intercalations (Fig. 4). Lenticular bodies with erosional bases and a fining upwards tendency were observed. However, the entire deposit exhibits a coarsening and thickening upwards tendency. Within the sandy bodies, the energy of the sedimentary structures increases towards the top, from planar cross-bedding (Sp), trough cross-bedding (St) and, finally, horizontal-lamination with parting lineation (Shh) (Fig. 8A). Syn-sedimentary deformation, such as convoluted lamination and load casts, was also recognized in this facies (Fig. 8B). The clast-supported conglomerates (Xmax 5 cm and X½ 1 cm) are lenticular with erosional bases. They exhibit planar cross-bedding (Gcp), trough cross-bedding (Gct) and sandy and tuff intraclasts up to 5 cm size (Gc_i). Laterally continuous, not-vegetated, volcaniclastic deposits are observed at the base of this facies. They correspond to a regional correlation level defined by González Bonorino and González Bonorino (1978) as "Miembro Tobas y Brechas" (MTB), here named as "green tuff" (Figs. 2 and 4). They are laminated tuffs (Tl) with soft-sediment deformation, which contain fossil flora remains. These levels are interbedded between coarse grained sandstones lenses which rework the volcanic material, exhibiting horizontal-lamination or low-angle cross--lamination (Sh, Sl), current-ripple cross-lamination (Sr) and planar cross-lamination (Sp).

The Facies 2 exhibits coarsening upward cycles between 2 and 4 m of thickness, which consist of sandstones and mudstones intercalations with high proportions of volcaniclastic deposits (Fig. 4). Tabular bodies of sandstones reworking the tuffaceous material were observed. Regarding the sedimentary structures, horizontal-lamination (Sh), planar cross-lamination (Sp), current-ripple cross-lamination (Sr) were identified. The bases are in general planar, but erosive bases were occasionally recognized. The thickness of the sand bodies increases towards the top. The mudstones, on the contrary, are more abundant in the base of the facies as thin levels interbedded among the sandstones, showing massive (Fm) and laminated (Fl) structures. The volcaniclastic deposits are mainly massive or laminated tuffs (Tm and Tl) interbedded

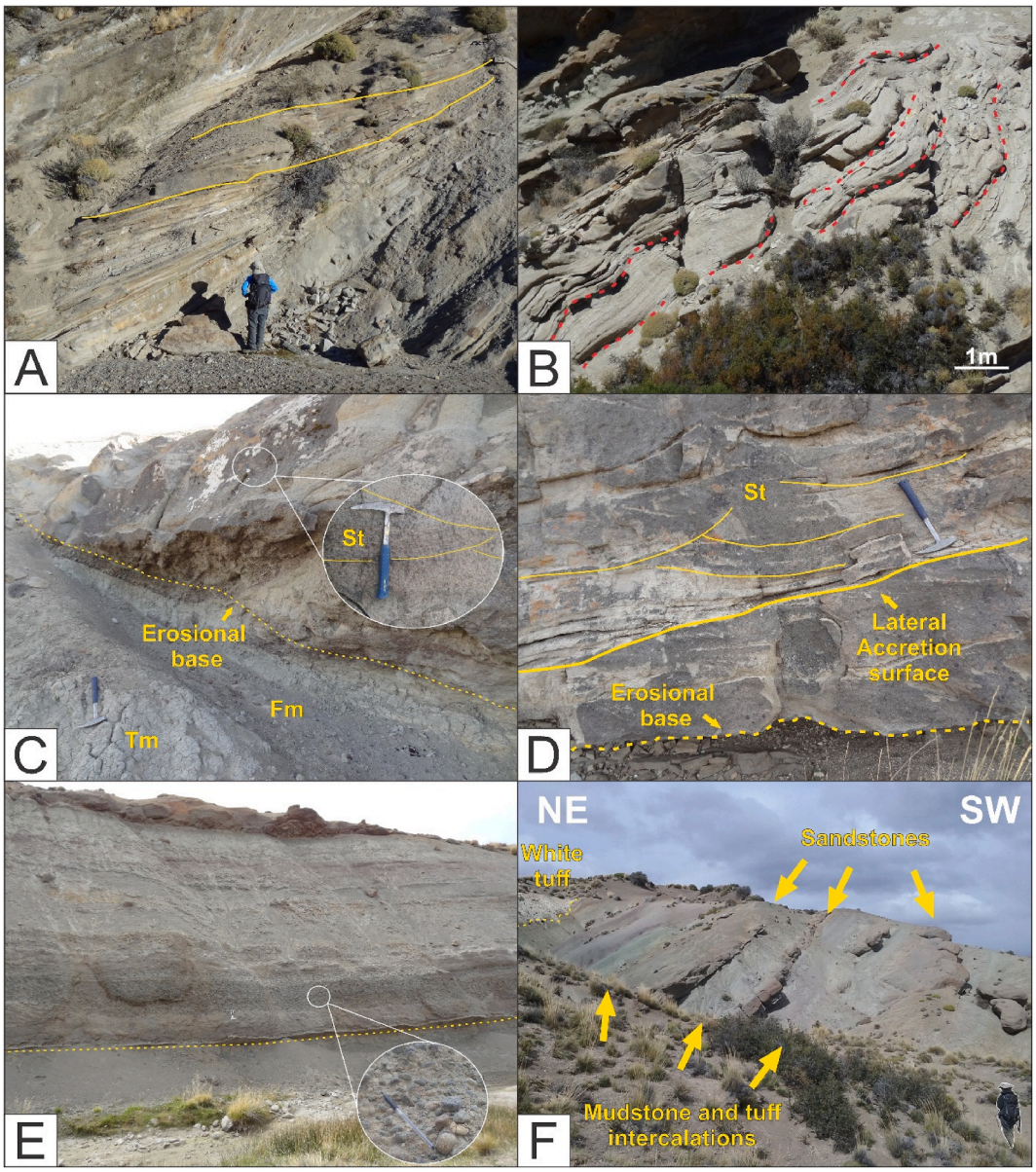

Fig. 8. Field photographs of the sedimentary facies observed in the Ñirihuau Formation (Facies Associations 5 and 6). A) Sandstones and conglomerates deposits of Facies 1 from FA5, with sedimentary structures evidencing transversal bar migration. B) Coarse to medium sandstone level with synsedimentary deformation (Facies 1 from FA5). C) Lenticular coarse-gravelly sandstone body with erosional base and trough cross-bedding (Facies 1 from FA6). D) Lateral accretion surface observed on tabular bodies of Facies 1 from FA6. Internal sedimentary structures of minor scale such as trough cross-bedding are observed on these deposits. E) Laterally continuous conglomerates with planar bases observed in Facies 1 from FA6, with rounded clasts; F) General aspect of the Facies 2 from FA6. Important thicknesses of greenish and purple mudstones are interbedded between tuffs levels and tuffaceous sandstones bodies.

between the sandstones.

Interpretation: The facies association 5 is interpreted as a fluvial system deposit with well-differentiated channel and inter-channel areas (Miall, 1996). The principal channels are constituted mainly by sand and gravel and the inter-channel area is constituted by important thicknesses of sand deposited as sheet flows with thin muddy levels, result of the final decantation (Tunbridge, 1981; Hampton and Horton, 2007). Due to the presence of lenticular bodies with erosional bases and fining upwards tendency, as well as the observed sedimentary structures (Gcp, Gct, Sp, St, Shh, Sh, Sl, Sr), Facies 1 is interpreted as channel deposits (Miall, 1996) with transversal bars migration. The presence of intraclasts in the coarser grained bodies (Gc_i) evidences the erosion of the inter-channel area deposits (Smith et al., 1989). The Facies 2 presents deposits of lower energy than the previous one. They are interpreted as sheet flows in the inter-channel area (Williams, 1971; Hogg, 1982), due to their tabular geometry and the observed sedimentary structures (Sh, Sp, Sr, Fm, Fl).

The facies association shows an important amount of explosive volcanic activity coetaneous with the sedimentation, represented by pyroclastic flows (Tl) and ash-fall deposits (Tm), in variable thickness bodies intercalated between the clastic facies. These periods of intense pyroclastic deposition are better registered in the inter-channel area, due to its lower energy (Smith, 1991).

5.6. FA6: Sandstones and conglomerates with mudstones

Description: The facies association 6 is constituted by conglomerates and sandstones with repeated intercalations of mudstones and high volcaniclastic participation. It was divided into two different facies according to the predominant lithology (Fig. 4). It is worth mentioning

that an outcrop showing a conspicuous lateral thickness variation was observed in this facies association (Fig. 6C).

The Facies 1 is constituted by conglomerates and sandstones. The conglomerates occur both in lenticular and tabular bodies with either erosive (Fig. 8C) or planar bases (Fig. 8E). They are clast-supported, with rounded to sub-rounded clasts of 3–4 cm in size, and planar (Gcp) and trough cross-bedding (Gct) structures. Pelitic and tuffaceous intraclast of great dimensions (up to 25 cm) (Gc) and concretions were also observed. The sandstone bodies exhibit lenticular and tabular geometries with erosional bases, the later shows, occasionally, lateral accretion surfaces (Fig. 8D). Their granulometry varies from coarse-gravelly to medium size and they constitute a fining and thinning upwards sequence. The observed sedimentary structures are through cross-bedding (St) where the sand is coarser; and planar cross-bedding (Sp), horizontal-lamination (Sh) and current-ripple cross-lamination (Sr) in the medium grained sandstones. In lower proportions, massive sandstones were also observed (Sm).

The Facies 2 is constituted by important thicknesses of mudstones interbedded with tuff levels and tuffaceous sandstones (Fig. 8F). The mudstones are laminated or massive (Fl, Fm) and are observed as tabular bodies of variable thicknesses (from 1 up to 50 m). Regarding the volcaniclastic deposits, there are massive tuffs and lapilli-tuffs (Tm, Tl). These levels exhibit abundant sandy intercalations with planar cross-bedding (Sp), trough cross-bedding (St) or current-ripple cross-lamination (Sr).

Interpretation: This facies association is interpreted as an anastomosed fluvial system (Makaske, 2001) that presents both braided and meandering channel complexes, with great thicknesses of floodplain deposits (Smith and Smith, 1980; Smith, 1986).

The Facies 1 is interpreted as channel deposits due to the sedimentary structures of unidirectional low regime fluid flow (Gcp, Gct, Sp, St, Sh, Sr, Sm) (Miall, 1996), and the intraclasts, which evidence erosion of the underlying pelitic alluvial floodplain (Gc_i) (Smith et al., 1989). As both lenticular and tabular geometries were observed, two cases were differentiated. In the first one, the multi-storey lenticular bodies are interpreted as braided channels (Miall, 1996). In the second case, the tabular bodies are interpreted as meandering channels due to its lateral continuity and the presence of lateral accretion surfaces (Miall, 1996).

The Facies 2, constituted by finer grained material, is interpreted as the alluvial floodplain deposits, with abundant volcaniclastic participation represented by ash-fall deposits (tuffs). In many cases these deposits are reworked, and this could be linked to ephemeral watercourses adjacent to the principal channels (Smith et al., 1989; Smith, 1991). In general, the tuffs are better preserved in this facies due to the fact that they are interbedded among lower energy deposits.

6. Sedimentary petrography

6.1. Sandstones

Thirteen samples of sandstones obtained from the stratigraphic section were analyzed for the petrographic characterization of the Ñirihuau Formation (Figs. 3 and 4). A total of 18 detrital constituents were identified in the petrographic analysis (Table 3).

The grain size of the samples varies from very fine to very coarse. Their texture is mainly clast-supported, and consists of angular to rounded grains, although there is a predominance of the sub-angular and sub-rounded ones, with a poor to moderate sorting. A variable compaction degree is evidenced by contacts between grains that varies from concave-convex to tangential, being the first ones only present near the base of the unit. The matrix is generally absent, and a small proportion of pseudo-matrix fills the intergranular space in some samples. Different types of cement occur, including chlorite, illite, zeolites, quartz, carbonates, and iron oxides. Porosity is generally low and was observed as both secondary (clast and cement dissolution) and primary intergranular.

According to the Folk et al. (1970) sandstone classification ternary diagram (Fig. 9A), the studied samples are mainly feldspathic litharenites and litharenites, with a minor proportion of lithic feldsarenites. Only one sample falls in the feldsarenites field. In general, lithoclasts are the most abundant component, followed by feldspars. However, in a few samples from the middle section, feldspars constitute the most abundant component (samples CÑ18, 459, 159 and CÑ38). Quartz is the least abundant component, and it increases its participation together with the feldspars.

In the provenance ternary diagrams (Dickinson et al., 1983; Dickinson, 1985) (Fig. 9B), the majority of the samples fall in the magmatic arc field, showing a supply of active continental margins related areas (subduction zones). All the samples from the lower section of the Ñirihuau Formation correspond to an undissected arc, reflecting the important contribution of lithic fragments and very low proportions of quartz (Dickinson et al., 1983; Dickinson, 1985). The samples from the middle section show more dispersion, as although they mainly fall in the transitional arc field, samples that correspond to the basement uplift, dissected arc, and undissected arc fields are also observed (Fig. 9B). The sample located in the basement uplift field (CÑ18) reflects a higher participation of feldspars, which in this case correspond almost entirely to plagioclase (Table 3). Samples from the upper section of the Ñirihuau Formation are located in the dissected arc field (CÑ38 and CÑ39), due to a higher participation of monocrystalline quartz and feldspars, and in the undissected arc field (CÑ41) due to an increase in the volcanic lithics participation in detriment of quartz and feldspars towards the top of the unit (Fig. 9B; Table 3).

To complement the study, the relationship between metamorphic, sedimentary and volcanic lithics was plotted in a ternary diagram (Fig. 9C). Samples CÑ08 and CÑ13, from the lower section of the unit, are slightly displaced towards the metamorphic lithics vertex, indicating a probable basement source in the base of the unit. Samples 458 and 459, from the middle section of the unit, are displaced towards the sedimentary lithics vertex reflecting a component of recycled basin fill. However, most of the samples are located in the volcanic lithics vertex due to the high participation of volcanic processes during sedimentation as well as the erosion of previous volcanic rocks.

The volcanic lithics with lathwork, microlithic and seriate to porphyritic textures (Lvl, Lvm, Lvs) were grouped as related to basic to intermediate volcanic rocks; while grainy, micrograiny (fine-grained), and devitrified textures such as spherulitic (Lvg, Lvmg, Lvd), were interpreted as related to acidic volcanic rocks. Monocrystalline quartz grains (Qm) with flash extinction are interpreted as mainly related to a volcanic and/or pyroclastic source or to basement granitic rocks, while those with enclosures are interpreted only as volcanic source. The potassium feldspar fragments (FK) can also be interpreted as coming from acidic volcanic and pyroclastic rocks, as well as from basement granitic rocks. Observed large, tabular, and frequently zoned plagioclase feldspars (Plg) reflect an basic to intermediate volcanic source, however basement granitic source could be also possible for the unzoned clasts. At the same time, the variable alteration degree of feldspars and, particularly, plagioclase, as well as the presence of pumice (Lvp) fragments indicates that there are both a primary volcanic source and a previous volcanic-sedimentary cycle source (Spalletti and Matheos, 1987). Therefore, the volcanic source of the Ñirihuau Formation detrital components is due to effusive and explosive events synchronic with deposition (especially pyroclastic, Spalletti et al., 1982) as well as to denudation of pre-existing lavas and pyroclastic rocks (Spalletti and Matheos, 1987). On the other hand, the metamorphic lithics (Lml, Lmh) represent a basement source, as well as the polycrystalline quartz with sutured contacts (Qps). However, polycrystalline quartz with straight contacts (Qpc) is interpreted as derived from recycled sedimentary lithics (chert). Sedimentary lithics (Lsm, Lsc) are also provided from a basin recycled sedimentary source but have a subordinated contribution in the studied stratigraphic section. As for the recognized accessory minerals (Acc), muscovite is interpreted as derived from granites or

Table 3
Detrital constituents recognized in the ten sandstone samples analyzed from the Ñirihuau Formation, 100% recalculated. References: FA: Facies Associations; Qm: monocrystalline quartz; Qpc: polycrystalline quartz with straights contacts (chert); Qps: polycrystalline quartz with sutured contacts; Plg: plagioclase feldspar; FK: potassium feldspar; Lvl: volcanic lithic with lathwork texture; Lvm: volcanic lithic with microlithic texture; Lvs: volcanic lithic with seriate texture; Lvg: volcanic lithic with grainy texture; Lvmg: volcanic lithic with micrograny texture; Lvd: volcanic lithics with devitrified textures; Lvp: pumice fragments; Lml: medium-grade metamorphic lithic; Lmh: high-grade metamorphic lithic; Lsm: Mudstone sedimentary lithic; Lsc: Carbonate sedimentary lithic (micritic); Lalt: Altered lithics; Acc: accessories.

Sample	FA	Latitude	Longitude	Qm (%)	Qpc (%)	Qps (%)	Plg (%)	FK (%)	Lvl (%)	Lvm (%)	Lvs (%)	Lvg (%)	Lvmg (%)	Lvd (g)	Lvp (%)	Lmm (%)	Lmh (%)	Lsm (%)	Lsc (%)	Lalt (%)	Acc (%)
CÑ06	1	41°28′35.42″S	71° 5′47.32″W	5.3	0.0	0.0	8.4	15.7	14.6	2.2	10.7	0.0	31.5	0.0	0.0	0.0	0.0	0.0	0.0	14.0	2.2
CÑ08	1	41°28′23.62″S	71° 5′40.67″W	2.4	2.9	2.9	6.7	11.5	20.1	14.4	3.8	3.3	5.3	2.4	0.0	1.0	3.3	0.0	0.0	13.9	6.7
CÑ11	2	41°28′21.28″S	71° 5′26.02″W	2.2	0.9	2.7	17.0	12.9	26.8	19.6	3.1	4.9	0.9	0.9	0.0	0.0	0.0	0.0	0.0	7.1	0.9
CÑ13	2	41°27′15.63″S	71° 5′42.40″W	4.5	2.1	2.6	13.9	8.8	26.8	12.9	3.6	6.7	3.1	2.6	0.0	0.0	0.5	0.0	0.0	10.8	4.1
CÑ16	3	41°27′13.00″S	71° 5′22.31″W	11.3	1.0	1.5	8.6	33.5	22.8	0.5	2.0	7.6	0.0	2.0	0.5	0.0	0.0	0.0	0.0	7.1	4.1
CÑ18	3	41°27′14.45″S	71° 4′43.00″W	30.8	0.6	0.0	58.1	16.2	4.8	1.8	0.0	1.2	0.0	0.0	0.0	0.0	0.0	0.0	0.0	1.8	3.0
459	3	41°27′13.33″S	71° 4′37.79″W	28.3	7.6	0.0	37.0	4.3	2.2	0.0	0.0	0.0	0.0	0.0	19.6	0.0	0.0	0.0	1.1	0.0	0.0
458	3	41°27′10.09″S	71° 4′34.19″W	5.5	0.0	5.5	11.0	4.1	8.2	5.5	0.0	0.0	24.7	0.0	13.7	0.0	0.0	21.9	0.0	0.0	0.0
CÑ31	3	41°26′52.40″S	71° 3′44.11″W	10.3	1.0	2.0	16.3	20.4	16.8	4.1	3.1	8.2	1.0	2.0	0.0	0.0	0.0	0.0	0.0	12.2	5.6
159	3	41°26′32.96″S	71° 3′11.55″W	18.0	1.1	0.0	48.3	1.1	13.5	0.0	0.0	0.0	3.4	7.9	6.7	0.0	0.0	0.0	0.0	0.0	0.0
CÑ38	5	41°26′25.67″S	71° 2′37.53″W	26.8	0.0	0.5	31.1	15.3	8.2	2.7	0.0	6.0	3.8	2.2	0.0	0.0	0.0	0.0	0.5	7.7	3.8
CÑ39	6	41°23′54.86″S	71° 4′39.73″W	33.5	0.0	2.6	24.7	18.8	10.4	2.6	7.1	5.8	1.9	2.6	1.3	0.0	0.0	0.0	0.0	9.7	2.6
CÑ41	6	41°23′58.19″S	71° 4′14.39″W	8.7	0.0	1.0	18.4	5.1	28.6	8.7	4.6	6.6	1.5	2.0	4.1	0.0	0.0	0.0	0.0	13.3	2.0

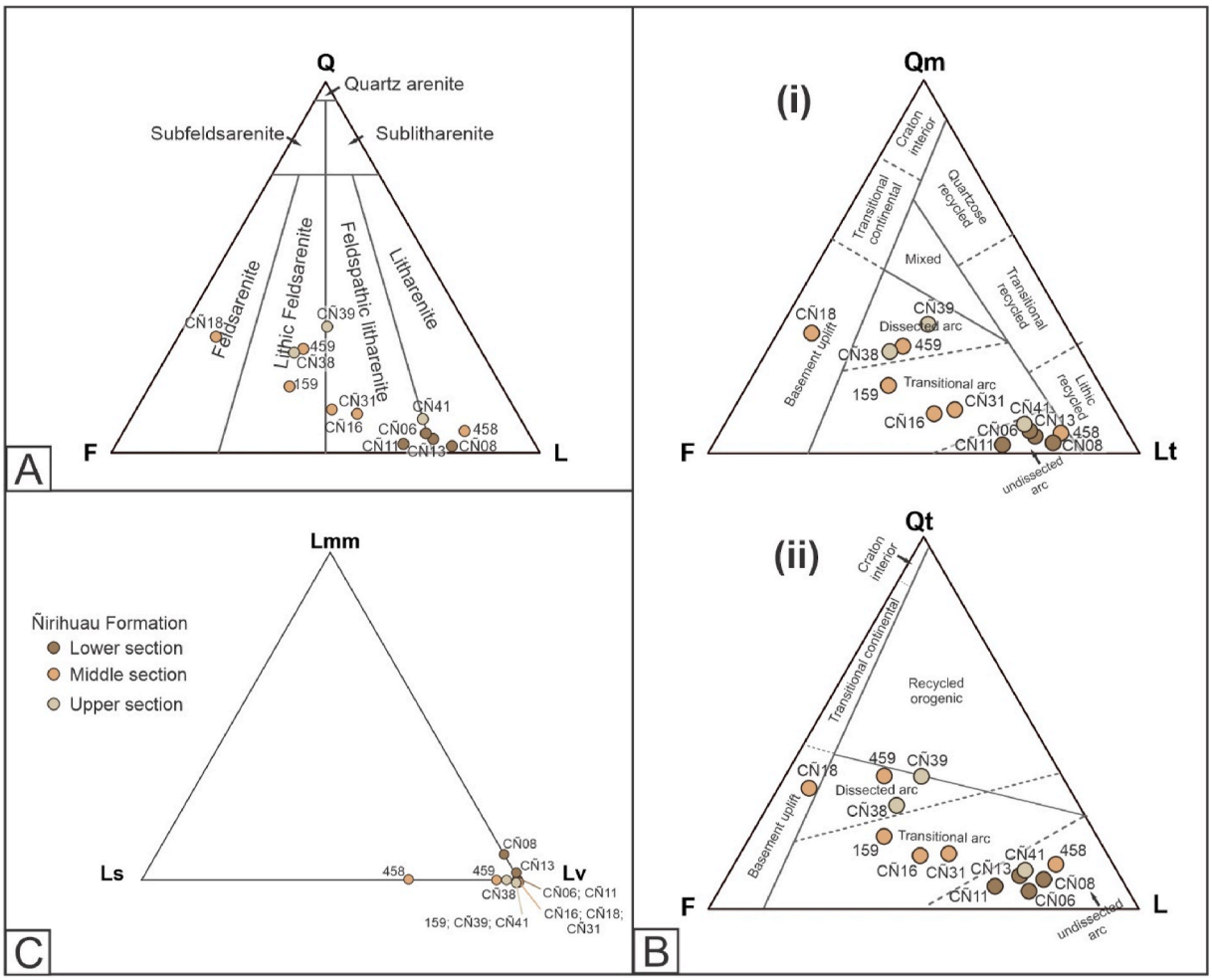

Fig. 9. A) Folk et al. (1970) ternary diagram illustrating petrographic classification of the ten sandstone samples analyzed from the Ñirihuau Formation. Q: Quartz; F: Feldspars; L: Lithic fragment. B) Dickinson et al. (1983) tectonic setting ternary diagrams (i and ii) illustrating petrographic variations of the Ñirihuau Formation sandstones to discriminate provenance areas. F: Feldspars; Lt: Total lithic fragments; L: Unstable lithic fragments; Qm: Monocrystalline quartz; Qt: Total quartz. C) Lithics ternary plot. Lmm: metamorphic lithics; Ls: sedimentary lithics; Lv: volcanic lithics.

metamorphic rocks (gneiss and schist) of the basement; while biotite could come from the volcanic sources or events, as well as pyroxene or amphibole clasts (Spalletti and Matheos, 1987).

According to the aforementioned, the components of basic to intermediate composition, plagioclase, and subordinate sedimentary detritus could come mostly from the erosion of the late Eocene to early Miocene magmatic arc of the El Maitén Volcanic Belt (Rapela et al., 1988) (Fig. 1). On the other hand, the Paleocene-Eocene Pilcaniyeu Volcanic Belt could be the source of the acidic elements (Fig. 1) (Rapela et al., 1988), although there are minor acidic intercalations in the El Maiten Belt that could be providing them as well (Fernández Paz et al., 2019). In a subordinate way, volcanic material could also come from the Jurassic volcano-sedimentary sequences located towards the west of the studied area (Fig. 1), which are compositionally similar to the Cenozoic volcanic belts (Giacosa et al., 2001). The few metamorphic lithics observed in the most basal section of the Ñirihuau Formation could derive from the Paleozoic igneous-metamorphic basement of the Colohuincul/Bariloche Complex (Basei et al., 1999; Varela et al., 1999; Oriolo et al., 2019), which closer outcrops are located to the west of the basin, as tectonic sheets limited by the backthrusts of the Cordón de Las Bayas (Fig. 2). In some cases, they can also come from the basin substrate, where the sedimentary rocks directly overlie the igneous-metamorphic basement, because of the wedging of the Ventana Formation towards the east (Mancini and Serna, 1989; Cazau et al., 1989). It should be mentioned that there is an important detrital contribution of primary volcanics (mainly pyroclastic), evidencing a synchronic volcanic activity during deposition of Ñirihuau Formation (Spalletti and Matheos, 1987).

Therefore, the main material contribution for the sandstones samples from the lower section of the Ñirihuau Formation (CÑ06 to CÑ13) is likely from the mentioned volcanic belts, due to the marked predominance of the volcanic lithics over other constituents (Table 3). The samples from the middle section of the unit (CÑ16 to 159) reflect an increase in the contribution of other constituents. However, the presence of basic to intermediate and acidic and volcanic lithics and pumice fragments as well as the predominance of plagioclase over potassic feldspar would indicate a provenance source from the erosion of the volcanic belts or from coetaneous volcanic eruptions. Finally, the samples from the upper section of the Ñirihuau Formation (CÑ38 to CÑ41) show an increase in the erosion rate due to the high participation of quartz and feldspars. However, volcanic lithics are also abundant reflecting the derivation from the volcanic belts or volcanic activity synchronic with sedimentation.

6.2. *Conglomerates*

Eight conglomerate clast counting was carried out along the Ñirihuau Formation, Two of them are located at the lower section of the unit but they do not belong to the studied stratigraphic section (CI and CII); the other ones, C1 to C6, are located along the studied stratigraphic section (Figs. 3 and 4). The sites are concentrated in the most basal

portion of the Ñirihuau Formation and near its top (lower and upper sections of the Ñirihuau Formation), due to the absence of conglomerate outcrops in the middle section of the unit. The types of rock fragments recognized in the field were grouped to follow a criterion similar to the one used for the sandstones analysis. Thus, basic to intermediate volcanic rocks include volcanic aphanitic clast with vesicles and fluidal textures, and porphyritic clasts with plagioclase feldspars and mafic phenocrysts; the acidic volcanic rocks correspond to acid clasts with porphyritic textures and potassic feldspar, quartz and plagioclase phenocrysts; and the metamorphic rocks include gneisses and schists clasts. Plutonic rocks with coarse grained texture, milky quartz, and vitric tuffaceous clasts were also identified (Table 4).

Basic to intermediate volcanic rocks clasts are the most abundant clast lithology along the unit, while acidic volcanic rocks clasts are only observed in very low proportions near its top (Fig. 10; C6). Tuff clasts are second in predominance, with higher concentrations at the base of the unit, and lower proportions towards the top. On the other hand, the metamorphic rocks, milky quartz, and plutonic rocks clasts are scarce and were observed mainly in the top of the lower section and, in lower proportions, near the top of the upper section (Fig. 10; CI, CII, C2, C4, C6).

The obtained results highlight a predominance of the basic to intermediate volcanic material contribution against the acidic and pyroclastic ones. These materials would have been contributed by the El Maitén Volcanic Belt and the Pilcaniyeu Volcanic Belt, respectively. It should be mentioned that the registered tuff clasts could be either reworked or related to volcanic eruptions synchronic with the sedimentation. The last case is the most common one, due to the homogeneous composition of the deposits and the angularity of the clasts. The fragments of medium to high-grade metamorphic origin (gneisses and schist clasts) were observed principally in the basal portion of the Ñirihuau Formation, but they were also identified towards its top, together with plutonic rocks (granitoids). Even though they are scarce, these clasts are the evidence of the source from the igneous-metamorphic basement, constituted by the Colohuincul/Bariloche Complex and the Subcordilleran and Cordilleran Patagonian Batholiths.

7. U–Pb zircon geochronology

Five sedimentary rocks (samples 156, 473, 474, 159, 467) and two tuff layers (samples 476, 468) were sampled for U–Pb in zircon provenance analysis (LA-ICP-MS); all samples belong to the studied Ñirihuau Formation section along the La Bayas creek (Figs. 3 and 4). These data were used to calculate the maximum depositional age (MDA) in the case of the sedimentary rocks, and the depositional age for the tuff samples (weighted average age) (Fig. 11).

For the MDA calculation of the sedimentary rocks samples two methods were considered, taking into account that the more data used, the more accurate the calculation is (Sharman and Malkowski, 2020). Both methodologies used in this study are the youngest graphical peak (YPP) and the youngest statistical population (YSP) (see Sharman and Malkowski, 2020 and references therein). The YPP is calculated as the youngest peak of a probability density plot and without an associated uncertainty. The YSP is the weighted mean of the youngest group of two or more analyses that have a mean square weighted deviation (MSWD) that is closest to one, which in the analyzed samples represent the YPP but with an associated uncertainty (Fig. 11). In all the analyzed samples,

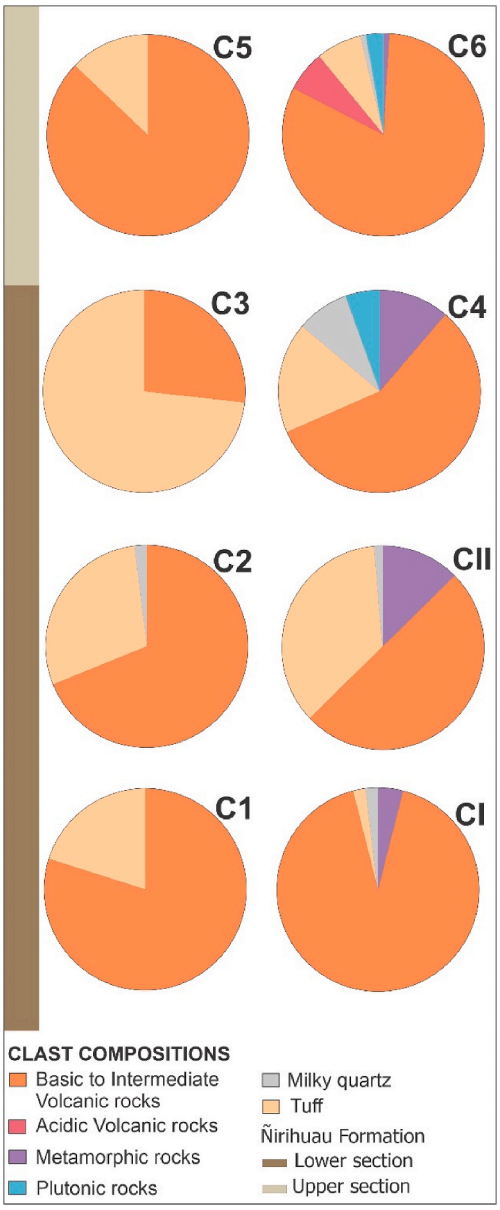

Fig. 10. Pie diagrams of the conglomerate clast counting carried out in the Ñirihuau Formation, showing the variation in the proportion of the different components identified along the studied stratigraphic section. See Figs. 3 and 4 for location.

Table 4
Rock fragments recognized in the eight clast countings from the Ñirihuau Formation, 100% recalculated. References: Lvb: Basic to intermediate volcanic rocks; Lva: Acidic volcanic rocks; Lmm; Metamorphic volcanic rocks; Lp: Plutonic rocks; Q: Milky quartz; T: Tuff.

Clast Counting	FA	Latitude	Longitude	Lvb (%)	Lva (%)	Lmm (%)	Lp (%)	Q (%)	T (%)
CI	–	41°27′46.24″S	71° 6′35.59″W	92.2	0.0	3.9	0.0	1.9	1.9
CII	–	41°27′37.79″S	71° 6′36.75″W	50.7	0.0	12.3	0.0	1.4	35.6
C1	1	41°28′35.50″S	71° 5′47.43″W	79.8	0.0	0.0	0.0	0.0	20.2
C2	1	41°28′23.62″S	71° 5′40.67″W	68.8	0.0	0.0	0.0	1.8	29.4
C3	2	41°28′15.98″S	71° 5′25.65″W	26.9	0.0	0.0	0.0	0.0	73.1
C4	2	41°27′20.29″S	71° 5′50.14″W	57.4	0.0	11.1	5.6	8.3	17.6
C5	6	41°23′57.07″S	71° 4′16.16″W	87.0	0.0	0.0	0.0	0.0	13
C6	6	41°24′12.51″S	71° 3′17.84″W	81.8	6.4	0.9	2.7	0.9	7.3

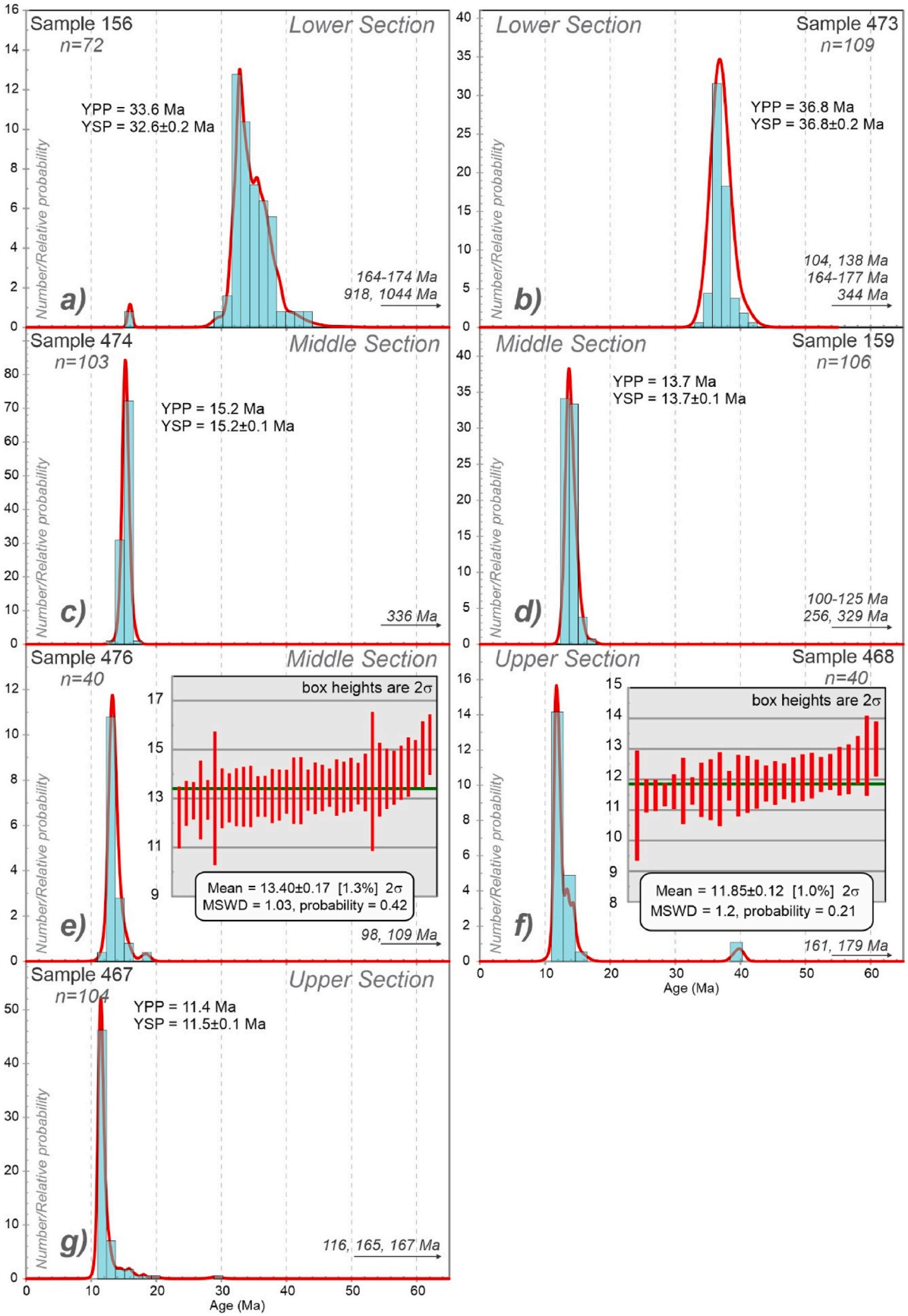

Fig. 11. Probability density plots and weighted average age diagrams for the analyzed samples, see text for detailed description of each sample. YPP: youngest graphical peak, YSP: youngest statistical population, MSWD: mean squared weighted deviation, n: number of zircons analyzed in each case.

the youngest populations of grains that delineate the YPP and YSP for the sedimentary rocks, or the weighted average age (WAA) for the tuff layers, have a Th/U relation higher than 0.2, suggesting a magmatic origin for the zircons.

7.1. U–Pb dating results

Sample 156 (FA1; sedimentary breccia; lower section): The YPP suggests a representative population of 33.6 Ma, and the YSP (n = 27) calculation suggests a MDA of 32.6 ± 0.2 Ma (MSWD = 1.05). Although the MDA is ca. 33 Ma, there is a youngest single grain dated on 16 Ma.

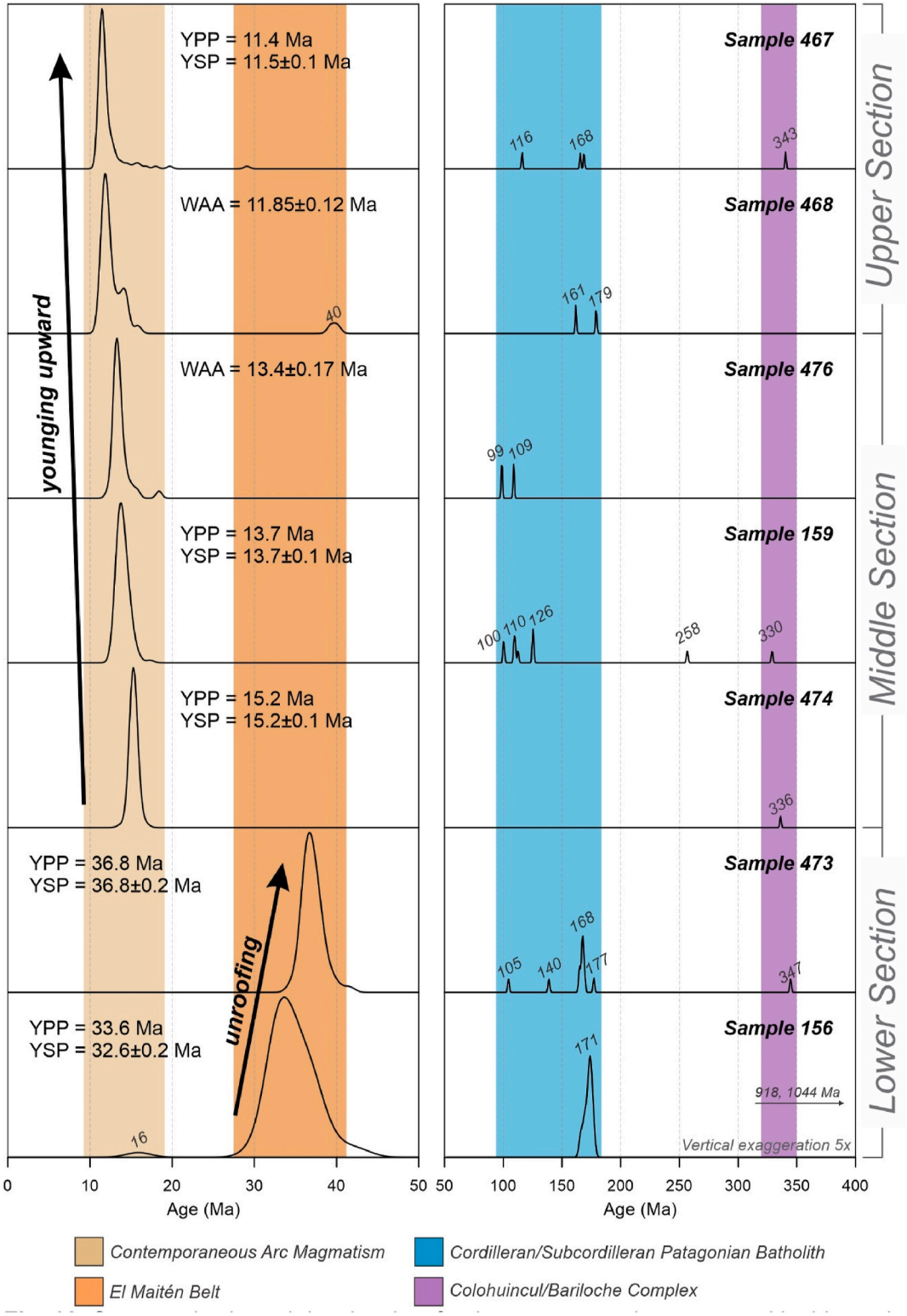

Fig. 12. Comparative kernel density plots for the seven samples presented in this study for the Ñirihuau Formation. Note that the vertical and horizontal scale is modified after 50 Ma. YPP: youngest probability peak, YSP: youngest statistical peak, WAA: weighted average age.

Other nine analyses have Jurassic ages between 164 and 174 Ma, and two older crystals have ages of 918 and 1044 Ma.

Sample 473 (FA2; sandstone; lower section): The YPP indicates that the youngest and most abundant population is about 36.8, with an YSP (n = 95) of 36.8 ± 0.2 Ma (MSWD = 1.00). Two analyses have Lower Cretaceous ages between 104 and 138 Ma, nine analyses show Jurassic ages between 164 and 177 Ma, and one older analysis of 344 Ma was also observed.

Sample 474 (FA3; sandstone; middle section): The analyses yielded an YPP of 15.2 and a YSP (n = 102) of 15.2 ± 0.1 Ma (MSWD = 0.8), which are interpreted as the MDA of the sample. Only one analysis has 336 Ma, suggesting a Carboniferous inheritance for this sample.

Sample 159 (FA3; sandstone; middle section): The YPP indicates a youngest population of 13.7 Ma, and the YSP (n = 87) is 13.7 ± 0.1 Ma (MSWD = 1.05), which is interpreted as the MDA of this sample. Nine inherited crystals have Lower Cretaceous ages between 100 and 125 Ma, one has a Permian age of 256 Ma, and the oldest one has a Carboniferous age of 329 Ma.

Sample 476 (FA3; vitric tuff (green tuff, "Miembro Tobas y Brechas"); middle section): The main population is about 13 Ma (n = 36), which delineates a weighted average age of 13.4 ± 0.1 Ma (MSWD = 1.03). Seven analyses have ages between 14 and 16 Ma, one has 18 Ma, and two have ages of 98 and 109 Ma.

Sample 468 (FA6; vitric tuff; upper section): The youngest population (n = 27) results in a weighted average age of 11.85 ± 0.1 Ma (MSWD = 1.2). Nine crystals represent a second population of 13–15 Ma, two other crystals have ages between 39 and 40 Ma, and the two oldest have Jurassic ages of 161 and 179 Ma.

Sample 467 (FA6; sandstone; upper section): The YPP suggests a representative population of 11.4 Ma, and the YSP (n = 84) calculation suggests a MDA of 11.5 ± 0.1 Ma (MSWD = 1.06). Sixteen analyses have ages between 13 and 29 Ma (Miocene-Oligocene), and one has Cretaceous age of 116 Ma, two older analyses have Jurassic ages of 165 and 168 Ma, and the oldest crystal has a Carboniferous age of 340 Ma.

7.2. Potential sediment sources interpretation

The potential discrete sediment sources recognized during Cenozoic basin evolution include (Figs. 1 and 12), from oldest to youngest: (1) a Precambrian to Paleozoic igneous-metamorphic basement constituted by the Colohuincul/Bariloche Complex, which is exposed both towards the west and east of the studied area (Varela et al., 2005; Pankhurst et al., 2006; Hervé et al., 2018); (2) Jurassic and Cretaceous plutonic rocks that constitute the Subcordilleran Patagonian Batholith and the Cordilleran Patagonian Batholith with outcrops to the west of the basin (Castro et al., 2011 and references therein); (3) Jurassic volcano-sedimentary sequences located towards the west of the studied area (Giacosa et al., 2001; Aragón et al., 2011), (4) the Paleocene to Eocene magmatic arc of the Pilcaniyeu Volcanic Belt located over the edge of the foreland to the east (42–60 Ma; Iannelli et al., 2017 and references therein); (5) the late Eocene to early Miocene magmatic arc of the El Maitén Volcanic Belt located in the subandean region to the west (previous U–Pb ages between 19 and 37 Ma; Aragón et al., 2011; Bechis et al., 2014a; Benedini et al., 2017; Fernández Paz et al., 2018, 2019); (6) cannibalized cenozoic sedimentary deposits; (7) detrital contribution of primary volcanism (mainly pyroclastic) synchronic with the deposition of Ñirihuau Formation, that could have been linked to the magmatism represented by the Miocene plutonic rocks of the Coluco Formation and equivalent units (7–19 Ma; Toubes and Spikermann, 1973; González Díaz, 1982; Rapela et al., 1988; Munizaga et al., 1988; Aragón et al., 2011).

Therefore, the results from the seven samples collected along the Ñirihuau Formation stratigraphic section exhibit five zircon sources (Fig. 12): (1) Precambrian; (2) Paleozoic (Carboniferous-Permian); (3) Mesozoic (Early Jurassic-Early Cretaceous); (4) late Eocene-Oligocene; (5) Miocene. Cenozoic zircons are largely predominant, while older sources are represented by only a few data. In all the analyzed samples, the identified sources evidence a dominance of sediment supply from areas located west of the basin.

8. Discussion

8.1. Age of the Ñirihuau Formation

The results obtained from the U–Pb LA-ICP-MS analyses suggest that deposition of the Ñirihuau Formation along the Arroyo Las Bayas might have started after the late Eocene. The two lower samples (156 and 473) exhibit maximum depositional ages (MDA) of 33 and 37 Ma respectively, showing a pattern of older upward ages (Fig. 12).These ages obtained for the lower section of the unit could represent provenance ages related to erosion of the underlying volcanic rocks (unroofing) of the El Maitén Volcanic Belt, where Fernandez Paz et al. (2019) recently obtained an U–Pb age of 33 Ma. Therefore, we consider that they are not representative of the true depositional age (TDA) of the samples.

Regarding sample 156, it has a youngest detrital zircon dated on 16 Ma (Fig. 11), which is much younger than the MDA of 33 Ma obtained for this sample. Dickinson and Gehrels (2009) suggested that the use of the youngest single detrital zircon (YSG) can be a measure of the youngest possible detrital zircon age, but inherent lack of reproducibility diminishes confidence in its reliability because some individual YSG ages might be spurious due to lead loss (see also Sharman and Malkowsky, 2020, and references therein). However, Dickinson and Gehrels (2009) support the use of the YSG when the source is actually close to the sampling site, as in the study case. The lack of an abundant population at ca. 16 Ma in sample 156 can be linked to an inadequate sediment supply (e.g., Sharman and Malkowsky, 2020). Additionally, the petrography of this breccia, with pumice and altered intermediate volcanic lithic clasts within a fined-grained devitrified vitreous matrix that overall shows an homogeneous recrystallized texture, suggests reworking, and not likely a primary volcanic deposit. Taking into account that the initial stage of the sedimentation of the Ñirihuau Formation is interpreted as related to an active tectonism (see the following section), the sediment supply of ca. 33 Ma could represent the main and closest source, El Maitén Volcanic Belt, but not a MDA close to the TDA. Then, a possible active distal volcanism could be the source of 16 Ma, but a rapid sedimentation of this facies and the high amount of local older zircons reduced the chance to preserve the youngest source, that in turn could hypothetically represent the TDA. This interpretation explains the gap between the MDA (not likely the TDA) of these basal breccias and the younger MDA obtained for the middle and upper sections (interpreted as the TDA), and also the fact that sample 156 shows younger ages than the overlying 473 sample (MDA ~36 Ma) (Fig. 12).

On the other hand, the younging upward pattern exhibited by the samples from the middle and upper sections (Fig. 12), together with the Th/U relations suggesting a magmatic origin for the analyzed crystals and the recognition of juvenile volcanic clasts in the petrographic analysis (Tables 3 and 4), can be interpreted as representative of the TDA of the analyzed sandstones (samples 474, 159, 467). Also, the two dated vitric tuffs are mainly composed of glass shards, pumices, and angular crystaloclasts, indicating that they correspond to primary ashfall deposits related to a contemporaneous volcanism (samples 476, 468). In this sense, to consider that the analyzed sandstones yielded an MDA close to the TDA, two fundamental requirements should be fulfilled (Sharman and Malkowski, 2020): i) there must be a contemporaneous volcanic source, and ii) the supply from that source must be much higher with respect to the supply of older sediments sources. In the case of samples 474, 159 and 467, the youngest populations are the most representatives and can be associated with the magmatic stage that generated the pyroclastic deposits of samples 476 and 468. This magmatism was probably related to the Miocene granitoids of the Coluco Formation and equivalent units (Fig. 1) (Toubes and Spikermann, 1973; González Díaz, 1982; Rapela et al., 1988; Munizaga et al., 1988; Aragón

et al., 2011). Thus, we interpret that the MDA of these sandstone samples are in turn their TDA, indicating that sedimentation of the Ñirihuau Formation occurred up to the early Tortonian (late Miocene).

Similarly, previous U–Pb geochronological studies in the Ñirihuau Formation are consistent with the results presented here. In the southeastern sector of the basin, the Ñirihuau Formation was constrained between 22 and 12 Ma (Ramos et al., 2015; Butler et al., 2020). Furthermore, Butler et al. (2020) obtained an older MDA of 37 Ma, but they do not consider it as a likely TDA for the Ñirihuau Formation. In the same locality, the overlying Collón Curá Formation was constrained between 13 and 9 Ma (Ramos et al., 2015; Butler et al., 2020; García Morabito et al., 2021), suggesting that the lower part of Collón Curá is coeval with the deposition of the upper section of the Ñirihuau Formation. Therefore, based on the available geochronological data for the Ñirihuau Formation along the basin, its deposition might have occurred exclusively in the Miocene, between 22 Ma (Aquitanian) and 11 Ma (Tortonian). The recent and more reliable U–Pb ages allow discarding previous K–Ar ages from tuffs intercalated in the middle and upper members of the Ñirihuau Formation, which ranged between 22 and 16 Ma (Cazau et al., 1989).

8.2. Tectono-sedimentary evolution

A four-stage tectono-sedimentary model for evolution of the Ñirihuau Formation in the Arroyo Las Bayas area is proposed, by integrating the sedimentary, provenance and geochronological data here presented (Fig. 13), and also, the data from previous studies on the Ñirihuau basin.

A foreland basin setting related to the propagation of an orogenic wedge and subsidence associated with the tectonic load, as suggested by Ramos and Cortés (1984) and Giacosa and Heredia (1999), was considered for the paleoenvironmental evolution of the analyzed stratigraphic section. However, the basal alluvial deposits constitute isolated outcrops with limited lateral extension, and the important thickness variations registered for the initial deposits of the Ñirihuau Formation along the basin, are more consistent with an initial deposition restricted to isolated depocenters distributed throughout the basin, and do not suggest a more extended sedimentation related to an eastward propagation of thrusting (Cazau et al., 1989; Mancini and Serna, 1989). Also, previous analysis of seismic lines from the studied area and from the southern sector of the basin have revealed that this initial infill is related to small depocenters limited by normal faults (Mancini and Serna, 1989; Giacosa et al., 2015; Bechis and Cristallini, 2006; Ramos et al., 2015; Orts et al., 2015). Furthermore, the important thicknesses (~600 m) of the lower alluvial section of the unit at the La Bayas section (FA 1 and 2), its coarse granulometry (clasts up to 0.5 m diameter size) and its local provenance, together with the abrupt facies transition towards the finer lacustrine deposits (FA 3) of the middle section, are not suitable with a typical foreland basin evolution. In such a setting, a coarsening upwards arrangement is expected due to the thrust belt propagation and shortening (DeCelles, 2012), similar to the one observed on the upper section of the unit. Instead, our new data are more consistent with a polyphasic basin evolution, with an initial infill related to an extensional stage, and an upper infill related to propagation of the Andean orogenic wedge, in agreement with the majority of the most recent interpretations (i.e. Mancini and Serna, 1989; Giacosa et al., 2015; Bechis et al., 2014a; Ramos et al., 2015; Orts et al., 2015).

8.2.1. Ñirihuau Formation lower section: Tectonic stage 1 (initial synrift)

The Ñirihuau Formation sedimentary record along the Arroyo Las Bayas starts with alluvial fan deposits conformed by conglomeratic braided channels dominated by longitudinal bars (FA1, Fig. 4). Overlying these deposits, a fluvial system conformed by sandy-conglomeratic braided channels dominated by transversal bars is registered (FA2, Fig. 4). Due to the decrease in the deposit's energy, they are interpreted as deposited in a distal alluvial fan or an axial river developed at the most distal portion of the fan. According to this interpretation, these depositional systems would be retrograding. These deposits are interpreted as a syn-extensional infill associated with small depocenters generated by normal faulting that affected the basin basement in the study area (stage 1: synrift initial stage; Figs. 13–15), which were observed in seismic lines described in previous works (Cazau et al., 1989; Mancini and Serna, 1989; Bechis, 2004; Bechis and Cristallini, 2006; Orts et al., 2015).

The sandstone samples analyzed from this lower portion of the unit (CÑ06 to CÑ13) fall in the undissected arc field (Fig. 9B) reflecting the important contribution of lithics fragments (mainly volcanic). The provenance analysis reveals a predominance of basic to intermediate volcanic lithics over other components (Table 3), that would come from El Maitén Volcanic Belt, which is located to the west and is constituted by basaltic andesites, andesites and dacites from the calc-alkaline series (Fernandez Paz et al., 2019). The scarce acidic volcanic material registered could have been provided by the Paleocene to Eocene Pilcaniyeu Volcanic Belt, located in the extra-andean zone (Fig. 1). However, since the U–Pb data from this section do not record populations of that age, these lithics could also be linked to the subordinate rhyolites and pyroclastic deposits registered in the El Maitén Volcanic Belt (Rapela et al., 1988; Fernández Paz et al., 2020). Metamorphic rock clasts have been observed both in sandstones (CÑ 08 and CÑ13; Table 3; Fig. 9C) and conglomerates (Fig. 10), and even though they are not predominant, they evidence a basement source probably related to the Colohuincul/Bariloche Complex, with closer outcrops located to the west of the basin (Figs. 1 and 2). This is compatible with the U–Pb geochronological results that show a few Precambrian to Paleozoic ages (Figs. 11 and 12). The tuff clasts registered in the conglomerates (Fig. 10), could reflect a pyroclastic supply synchronic with sedimentation as well as products of the erosion of the Ventana Formation pyroclastic deposits (Fernandez Paz et al., 2019). This process is also evidenced by the late Eocene-Oligocene peaks from geochronological analysis for the most basal levels (samples 156, 473), that show an older-upwards ages pattern, interpreted as unroofing of the previous volcanic unit during the initial stages of sedimentation, induced by normal faulting related to the extensional tectonics (Fig. 12).

8.2.2. Ñirihuau Formation middle section: Tectonic stages 2 (synrift climax and declination) and 3 (transitional phase)

This stage is represented by the development of a lacustrine system (FA3, Fig. 4), with fine-grained deposits of middle Miocene ages (>15 Ma; Figs. 11 and 13), which exhibit great vertical development, and are affected by normal faulting (Fig. 6A and B). A shallow lacustrine system was first established, which was later followed by deeper lacustrine facies (Figs. 4 and 13). We interpret that this initial lacustrine system was formed in the hanging wall of an important normal fault, during a period of fault interaction and linkage (early stage 2: synrift climax), which would have produced the deepening and enlargement of the depocenter (Gawthorpe and Leeder, 2000). The main active faults during this period could have been located to the west, where west-vergent thrusts related to the later shortening (Las Bayas Backthrusts; Bechis et al., 2014a) could have been formed by inversion of previous east-dipping normal faults (Fig. 15).

A depositional system progradation is later registered (15.2 Ma), observing a new somerization in the lacustrine system due to a decrease in the accommodation space, that finished with the progradation of Gilbert-type deltas over the lacustrine sediments (FA4; Figs. 4, 7 and 13). This could correspond to the synrift final stage, related to deactivation of the main border fault (Gawthorpe and Leeder, 2000) (late stage 2: synrift final stage; Figs. 13–15).

Between ~15 and 13.4 Ma, the deltaic system was covered by laminated fine-grained deposits that correspond to a medium to shallow deep lacustrine system. These lacustrine deposits exhibit a greater areal extension than the first ones registered and contain microfossils that could indicate a brief sea connection during the sedimentation (Mancini

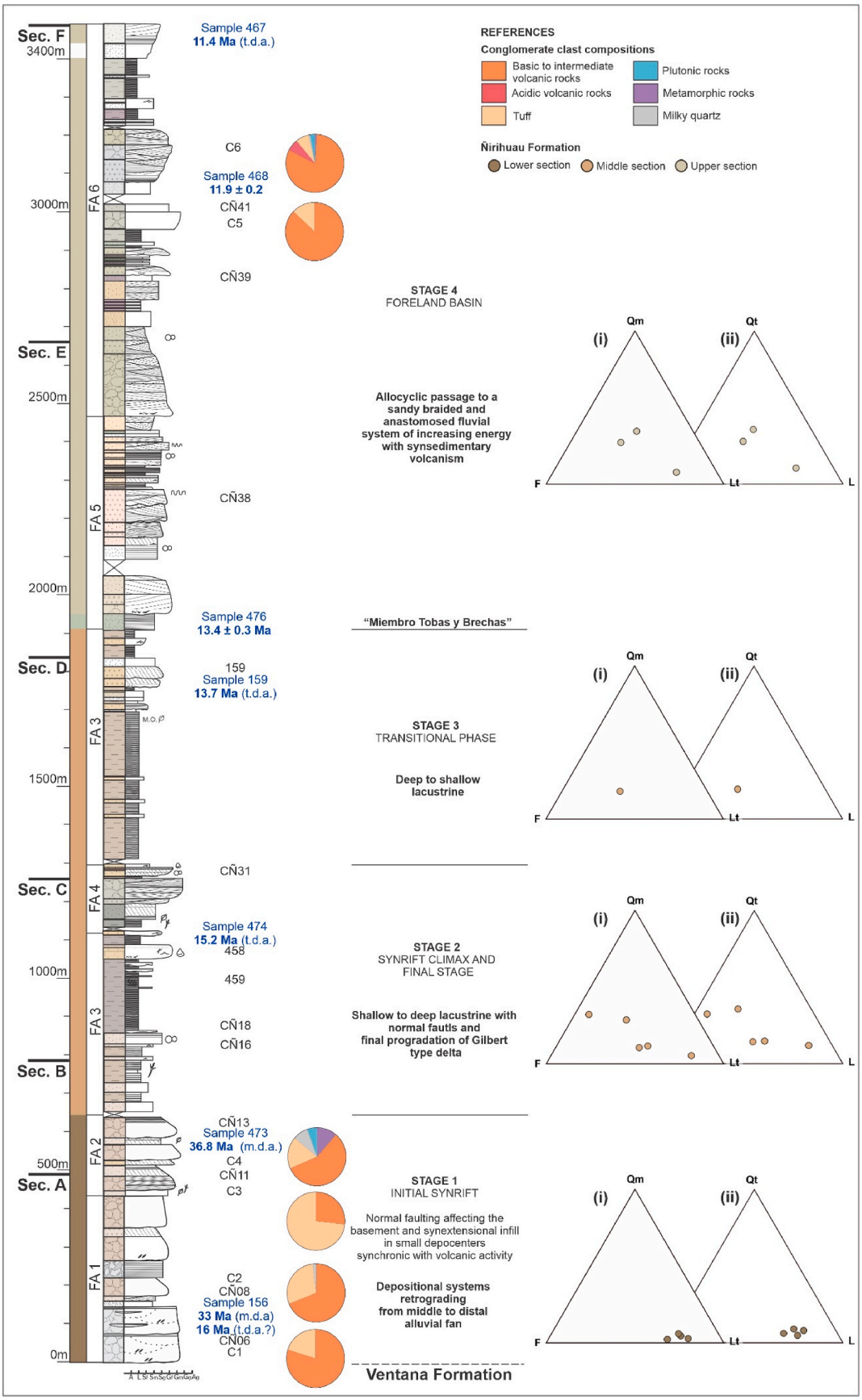

Fig. 13. Synthetic stratigraphic section of the Ñirihuau Formation along the Arroyo Las Bayas (see Fig. 4 for references). Ñirihuau Formation's paleoenvironments, age distribution and the main stages in the interpreted tectono-sedimentary evolution are indicated. Results of the sedimentary petrography analysis are also shown (see Fig. 9 for Dickinson ternary diagrams' references).

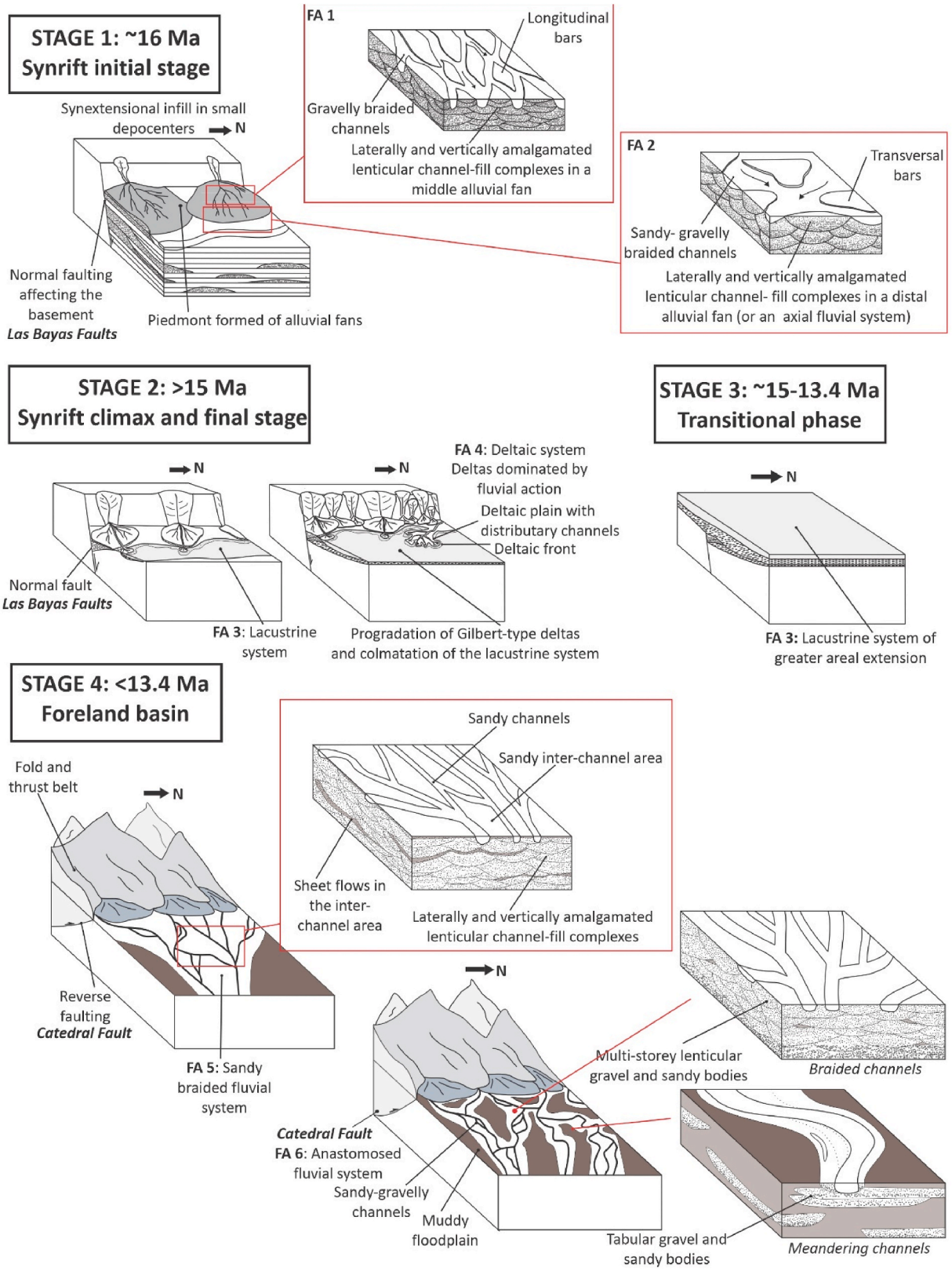

Fig. 14. Local schematic illustration of the proposed tecto-sedimentary evolution model for the Ñirihuau basin at the Arroyo Las Bayas area during the deposition of the Ñirihuau Formation. The synrift, transitional and foreland basin stages and the associated variation in the sedimentary environments are represented.

and Serna, 1989; Cazau et al., 1989).This new pulse of widespread increase in the accommodation space could have been controlled by thermal subsidence or by a tectonic load related to the beginning of compression and thrusting in the western sector of the Patagonian Andes (stage 3: transitional phase; Figs. 13–15).

A new pulse in the volcanic activity is later registered at 13.4 Ma (Sample 476; Fig. 11), reflected in the incorporation of ash-fall deposits (green tuff) which cover the fine-grain lacustrine facies. These ash-fall

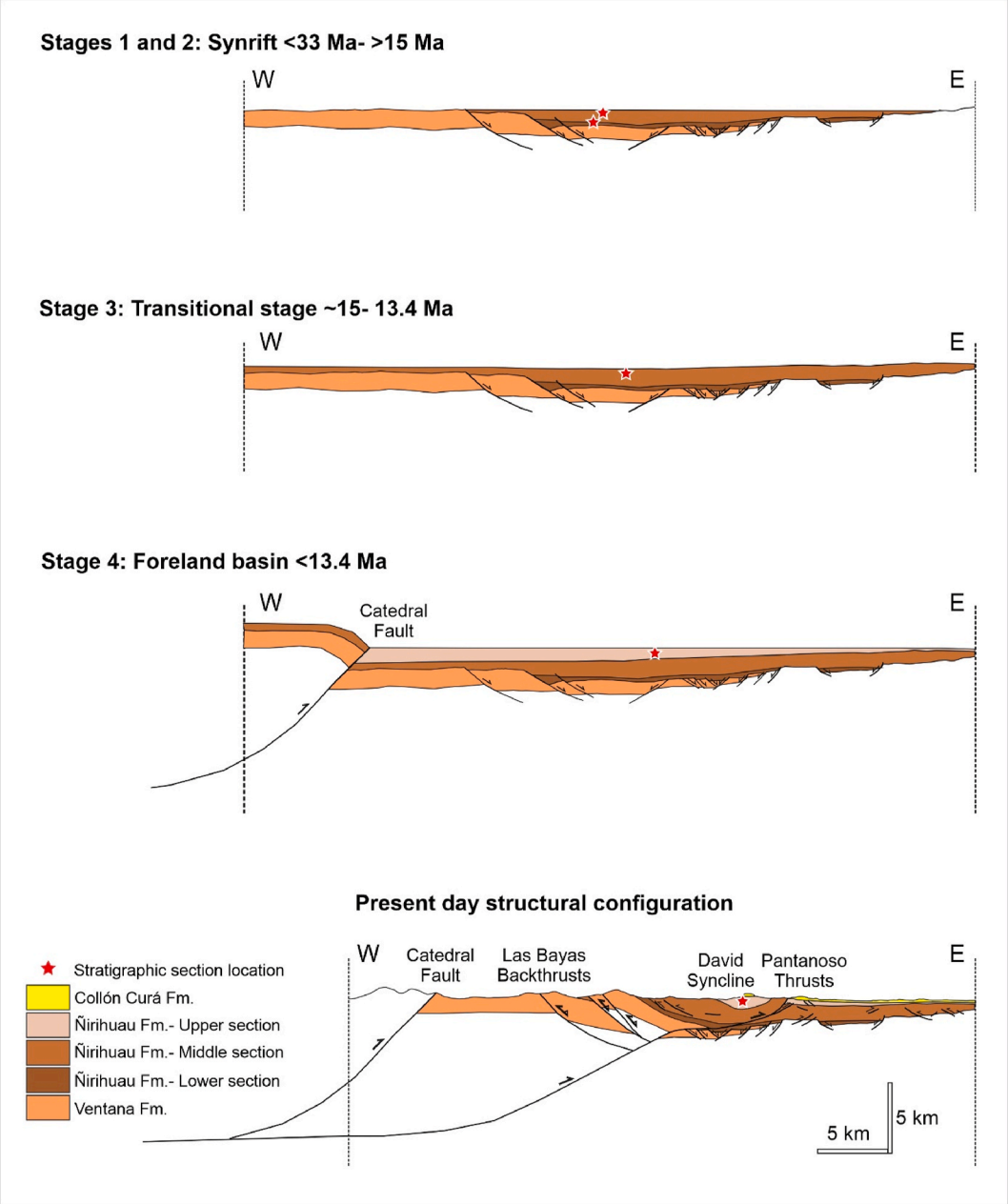

Fig. 15. Schematic cross-sections illustrating the different tectono-sedimentary stages proposed in this work for the Arroyo Las Bayas area (the present-day cross-section is based on Bechis et al., 2014a and Orts et al., 2015). The main structures and the distribution of the related depositional facies are represented. See Fig. 1 for location.

deposits are laterally correlated with coarser pyroclastic breccias (Bechis, 2004), all of which are part of the "Miembro Tobas y Brechas" defined by González Bonorino and González Bonorino (1978), which is a conspicuous marker bed for the northeastern sector of the Ñirihuau basin (Figs. 2 and 3).

In the lacustrine middle section of the unit, the sandstone provenance analysis revealed a greater participation of feldspars (Table 3). This could be indicating a granite source and it is reflected by a transition from the undissected arc field into the basement uplift field, going through the transitional arc field (Fig. 9B). However, volcanic lithics, and mainly the basic to intermediate ones, are still abundant (Table 3), suggesting that the material would still be provided by El Maitén Volcanic Belt to the west or by effusions synchronic with sedimentation. The sample located in the basement uplift field (CÑ18) reflects more participation of feldspars, and particularly plagioclase, rather than lithic fragments. This is commonly assigned to areas of high relief related to extensional and pull-apart basins (Dickinson, 1985; Tucker, 2009), but it could also correspond to foreland basins related to fold and thrust belts or as a response to the intense erosion of the magmatic arc, resulting in the exhumation of granitic rocks and the consequent dominantly quartz-feldspathic, lithic-poor sands. However, in all those cases, a higher participation of alkaline feldspar, instead of plagioclase, would be expected (Table 3). Therefore, due to its composition and stratigraphic position, the presence of plagioclase could be related to erosion of the previous volcanic units during the early synrift stage. It should be noticed that sample 458 falls into the undissected arc field (Fig. 9B) as a consequence of a higher participation of sedimentary lithics (mudstone intraclasts), as well as the volcanic lithics contributed by the volcanic belt. An increase in the acidic volcanic rocks participation observed towards the younger lacustrine deposits (Table 3), could be reflecting a

contribution from the Pilcaniyeu Volcanic Belt, located to the east of the basin (Fig. 1). But, as the U–Pb geochronology results for this middle section do not show ages of the Pilcaniyeu Volcanic Belt, these volcanic lithics could be assigned to the minor amount of rhyolites from the El Maitén Volcanic Belt or to the arc magmatism synchronic with the basin. Minor populations of Paleozoic and Middle Jurassic to Early Cretaceous ages could be derived from other sources such as the Colohuincul/Bariloche Complex and the Subcordilleran and Cordilleran Patagonian Batholiths, located westwards (Fig. 12). On the other hand, the younger and mayoritary Miocene age populations could be linked to the contemporaneous magmatic arc, as well as to the erosion of the basin deposits (Fig. 12).

8.2.3. Ñirihuau Formation upper section: Tectonic stage 4 (foreland basin)

Finally, from 13.4 to 11.4 Ma, a sandy braided fluvial system that presents synsedimentary volcanism was developed in the upper section of the unit (FA5, Figs. 4 and 8). At this moment, an abrupt facies change occurred, as higher energy deposits are registered, and syn-sedimentary deformation such as convoluted lamination and load casts is abundant (Fig. 8B). We interpret this transition as related to the advance of the orogenic front, combined with an important pyroclastic supply, and the consequent deposition of the synorogenic wedge in the foreland basin system (stage 4; Figs. 13–15). The upper levels of the basin infill show a progressive increase in the fluvial system energy, evidenced by a coarsening upwards tendency, that could have been probably linked to the fold and thrust belt development to the west of the basin, during the middle Miocene (<13.4 Ma). These deposits correspond to an anastomosed fluvial system, constituted by both braided and meandering channels, with great development of muddy floodplains (FA6, Fig. 4). This indicates an increase in the accommodation space, that we interpret to be related to subsidence generated by the tectonic load of the blocks raised by thrusts towards the west (Catedral Fault; Fig. 15). The lateral thickness variation observed in outcrops assigned to the Facies Association 6 (Fig. 6C) suggests that folding of these beds was already active during its deposition, as the strata show a conspicuous thickening towards the east, where the axis of the David syncline is located (Fig. 3B). Then, these growth strata are an evidence of deposition occurring simultaneously with deformation, probably during the wedgetop stage of the foreland basin.

According to the sandstone petrographic provenance analysis, in this upper portion of the unit the material could still be provided by the El Maitén volcanic belt (Fig. 1) due to the high volcanic contribution (Table 3). Pumice fragments participation is also registered towards the top of the unit (CÑ41), indicating an increasing contemporaneous volcanic activity (undissected arc field; Fig. 9B). However, two of the sandstone samples from the upper section (CÑ38 and CÑ39) fall into the dissected arc field, due to an increase of feldspars and quartz in detriment of lithic fragments (Fig. 9B; Table 3). Metamorphic and plutonic lithics are registered in the conglomeratic facies (Fig. 10), indicating a basement source that could be related to the compressive deformation that facilitated the uplift and erosion of blocks. The results obtained from the U–Pb zircons dating are dominated by young Miocene ages, much of which are syndepositional or shortly pre-depositional, and only a minor provenance from the Paleozoic and Mesozoic metamorphic and plutonic rocks is recorded (Fig. 12). Miocene ages populations older than the youngest peak could also be reflecting the cannibalization of the Cenozoic sedimentary deposits (Fig. 12). Therefore, the magmatic arc was the dominant source of sediment, masking older sources in the geochronological data. However, these older sources, although subordinate, are clearly registered in the sandstone petrographic analysis and conglomerate clast counting.

8.3. Regional considerations

We interpret that the analyzed data from the Ñirihuau Formation deposits reflect a transition from extensional to mainly syn-orogenic conditions. In the studied stratigraphic section, this tectonic regime transition would have taken place in the middle Miocene (~15–13 Ma).

The interpreted extensional stage during the deposition of the alluvial deposits from the lower section of the unit (stage 1: initial synrift; FA1 and 2; Figs. 13–15) could be related to the extension that favored the marine transgression registered in the Río Foyel and Troncoso formations (El Foyel Group) in the El Bolsón Basin (Fig. 1) (constrained between 22 and 16 Ma; Bechis et al., 2014). This is roughly contemporaneous with deposition of marine beds intercalated in the youngest section of the Ventana Formation (El Maitén Volcanic Belt) (Fig. 1) (23–19 Ma; Bechis et al., 2014; Fernández Paz et al., 2019, 2020). Alternatively, the extension in the Arroyo Las Bayas sector could correspond to a renewed extensional pulse.

Paredes et al. (2009) proposed that the El Bolsón and Ñirihuau basins were connected as a single large basin during the early stages of deposition of the Ñirihuau Formation. They interpreted that the deposition of the conglomerates from the most basal section of the Ñirihuau Formation were deposited next to a very local structural high. However, the available data are more consistent with a sedimentation in normal fault bounded, relatively isolated depocenters (Stage 1, Fig. 15), as it is observed on seismic lines data from previous contributions (Mancini and Serna, 1989; Giacosa et al., 2015; Bechis and Cristallini, 2006; Bechis et al., 2014; Ramos et al., 2015; Orts et al., 2015). In the El Bolsón basin Bechis et al. (2014a) suggested that the extensional conditions would have lasted until the late early Miocene (~16–17 Ma), as they observed growth strata associated to normal faults affecting the Troncoso Formation (Fig. 1). Also, progressive unconformities associated with normal faults were described for volcanic sequences dated at ~15 Ma in the Cerro Silvia, which is part of the Cordón Hielo Azul, a range located west of the El Bolsón Village (Fig. 1) (Tobal et al., 2015). Together with our interpretation, these previous data suggest that regional extensional conditions could have lasted until the early middle Miocene. On the other hand, some previous works interpreted that the compressional tectonic setting was already established during the early Miocene, based on the interpretation of syntectonic growth strata (Orts et al., 2012; Bilmes et al., 2013; Ramos et al., 2015). The contrasting interpretations for the beginning of the Andean shortening in the North Patagonian Andes suggest that more evidence is needed in order to unravel the regional tectonic setting during this period.

According to the thickness of the studied stratigraphic section (about 3500 m) and the ages that comprise the unit (>15 to 11 Ma), an overall high sedimentation rate is registered. Particularly, the predominance of lacustrine deposits observed in the middle part of the studied section (FA3, Fig. 4), evidences that the relation between the accommodation rate and the material contribution rate was greater than 1 (Paredes et al., 2009). The lake expansion and contraction cycles reflect the relationship between the material contribution rate and the generation of accommodation space. Due to the fact that the lacustrine system persisted even after great volcaniclastic material incorporation during a syn-eruptive stage, Paredes et al. (2009) suggested a high subsidence rate for the basin, with an increasing accommodation space, which favored the preservation of the volcanic deposits registered in the studied stratigraphic section. This high subsidence could be related to the extensional processes that were affecting the basin during its deposition (Stage 2: synrift climax and declination; Fig. 13).

The second lacustrine stage registered on the middle section of the unit represents a transitional phase between the extensional and compressional regimes (Stage 3: ~15 to 13 Ma; Fig. 15). According to Cazau et al. (1989) and Mancini and Serna (1989), this lacustrine system was more areally extended than the first one. This is a potential moment of higher connection between the different depocenters of the region, representing either the thermal cooling after the rifting or the start of Andean shortening to the west of the basin.

Finally, from 13.4 Ma onwards, during deposition of the upper section of the unit, fluvial systems developed under a compressive regime (FA5 and FA6, Fig. 4; Stage 4: foreland basin; Fig. 13) as was already

interpreted in previous publications (Cazau et al., 1989; Mancini and Serna, 1989; Spalletti and Dalla Salda, 1996). In the study area, frontal propagation of the fold and thrust belt would have incorporated the basin deposits in the deformation during deposition of its uppermost infill, which was previously interpreted as coeval with the activity of the Pantanoso thrust and the related wide David syncline (Fig. 15) (Paredes et al., 2009; Giacosa et al., 2005). This deformation, in turn, would have produced the uplift of basement blocks that ended up disconnecting the El Bolsón and Ñirihuau basins (Paredes et al., 2009; Bechis et al., 2014a).

9. Conclusions

An integrated study of the Ñirihuau Formation was carried out in one of its thicker and best exposed sections, located along the upper course of the Arroyo Las Bayas. An important body of new sedimentologic and geochronologic data were combined in a tecto-sedimentary model for the evolution of the Ñirihuau basin in the studied area, including an initial extensional stage, followed by a transitional phase and a final foreland basin stage, related to the Andean shortening.

A sedimentary and stratigraphic section of a total thickness of 3500 m of the Ñirihuau Formation was obtained. The unit was characterized according to its lithology, sedimentary structures, bodies geometries, and fossil content. Six facies associations were recognized (FA1 to FA6) reflecting the depositional paleoenvironment variations. Deposits related to volcanic events contemporary with the sedimentation were repeatedly recorded.

FA1 and FA2, interpreted as a medium to distal alluvial fan deposits or an axial fluvial system developed in the most distal part of an alluvial fan, were identified in the lower section of the unit. They were interpreted as a sinextensional infill in small depocenters generated by normal faulting during the initial synrift stage. The middle section of the unit is constituted by lacustrine sediments of FA3 and by a deltaic system registered between the two lacustrine deposits, which corresponds to FA4. In this section, the synrift climax and declination and a transitional stage were recognized. Deposition during the transitional stage could be either related to a post-rift thermal subsidence or to the start of the Andean building to the west. Finally, higher energy deposits corresponding to fluvial systems registered in FA5 and FA6 constitute the upper section of the unit. They were deposited during the foreland basin stage, related to the advance of the fold and thrust belt.

A detailed provenance analysis was carried out on the basis of sandstone petrographic studies, conglomerate clast counting, and detrital zircon U–Pb LA-ICP-MS geochronology. A basic to intermediate volcanic rocks supply is predominant at the base and top of the unit, and an important input of pyroclastic material is registered in the middle and upper sections. The main identified sediment sources correspond to volcanic events synchronic with the deposition of the Ñirihuau Formation and volcanic rocks from the El Maitén Volcanic Belt. Minor contributions from the Colohuincul/Bariloche Complex, Cordilleran and Subcordilleran Patagonian Batholiths, and recycled Cenozoic sedimentary deposits of the basin were also registered. Therefore, the main sediment sources are located to the west of the basin.

Finally, the new U–Pb geochronological data suggest that deposition of the Ñirihuau Formation in the Arroyo Las Bayas occurred mostly within the middle to late Miocene. The middle and upper sections were constrained between 15 and 11.4 Ma (Langhian to Tortonian). The basal deposits show Eocene maximum depositional ages, which were interpreted as related to erosion of the underlying volcanic rocks, while a possible middle Miocene age (~16 Ma) for this lower section was discussed.

Credit author statement

Camila Santonja Conceptualization, Main field work, Investigation, Methodology, Writing – original draft, Visualization. Florencia Bechis Conceptualization, Main field work, Investigation, Methodology, Writing – review & editing, Supervision. Project administration, Funding acquisition. Julieta Suriano Conceptualization, Main Field work, Investigation, Methodology, Writing – review & editing, Supervision. Juan I. Falco Conceptualization, Investigation, Methodology, Writing – review & editing. Alfonso Encinas Conceptualization, Investigation, Writing-review & editing, Funding acquisition. Ezequiel R. Olaizola Writing-review & editing. Victor A. Valencia Writing-review & editing, Methodology, Resources, Supervision. Vanesa D. Litvak Writing-review & editing, Resources, Supervision. Victor A. Ramos Writing-review & editing, Resources, Supervision, Funding acquisition.

Declaration of competing interest

The authors declare that they have no known competing financial interests or personal relationships that could have appeared to influence the work reported in this paper.

Acknowledgements

This research was funded by Universidad de Buenos Aires (geology student grant), Agencia Nacional de Promoción Científica y Tecnológica (PICT-2014-2240, PICT-2017-3259 and PICT-2018-2356 projects) and Universidad Nacional de Río Negro (40-B-743 project). AE was founded by Conicyt, Fondecyt projects 11080115, 1110914, and 1151146. We wish to give special thanks to Barbara Vera, Sergio Orts, Donald Bran and Maisa Tunik for their invaluable help in the field. We also thank Darío Lazo por helping with the identification of the bivalves' fossils, and Sofía Bordese (LA.TE. ANDES) for conducting part of the U–Pb analyses. Finally, the editor, Sébastien Carretier, and the reviewers, Patrice Baby and Brian Horton, are sincerely thanked for their constructive and helpful comments and suggestions which considerably improved the original manuscript.

Appendix A. Supplementary data

Supplementary data to this article can be found online at https://doi.org/10.1016/j.jsames.2021.103487.

References

Aguirre Urreta, M.B., 1992. Tertiary freshwater decapada (crustácea: Parastacidae) from the Ñirihuau basin, Patagonia, Argentina. J. Paleontol. 66 (5), 817–825.
Aragón, E., Mazzoni, M.M., 1997. Geología y estratigrafía del complejo volcánico piroclástico del río Chubut medio (Eoceno), Chubut, Argentina. Rev. Asoc. Geol. Argent. 52 (3), 243–256.
Aragón, E., Romero, E., 1984. Geología, paleoambientes y paleobotánica de yacimientos terciarios del occidente de Río Negro. Actas 9° Congreso Geológico Argentino, Buenos Aires, pp. 475–507.
Aragón, E., D'Eramo, F., Castro, A., Pinotti, L., Brunelli, D., Rabbia, O., Rivalenti, G., Varela, R., Spakman, W., Demartis, M., Cavarozzi, C., Aguilera, Y., Mazzucchelli, M., Ribot, A., 2011. Tectono-magmatic response to major convergence changes in the North Patagonian suprasubduction system; the Paleogene subduction-transcurrent plate margin transition. Tectonophysics 509 (3–4), 218–237.
Aragón, E., Castro, A., Diaz-Alvarado, J., Pinotti, L., Fernando, D., Demartis, M., Coniglio, J., Hernando, I., Rodriguez, C., 2018. Mantle derived crystal-poor rhyolitic ignimbrites: eruptive mechanism from geochemical and geochronological data of the Piedra Parada caldera, Southern Argentina. Geoscience Frontiers 9 (5), 1529–1553.
Adriasola, A.C., Thomson, S.N., Brix, M.R., Hervé, F., Stöckhert, B., 2005. Postmagmatic cooling and late cenozoic denudation of the north patagonian Batholith in the los Lagos region of Chile, 41°-42°15'S. Int. J. Earth Sci. 95, 504–528.
Allmendinger, R.W., Cardozo, N., Fisher, D., 2012. Structural Geology Algorithms: Vectors and Tensors in Structural Geology. Cambridge University Press, Cambridge.
Asensio, M., Cornu, M., Malumián, N., Martínez, M., Quattrocchio, M., 2010. Formación Río Foyel, Oligoceno de la Cuenca de Ñirihuau: la transgresión pacífica en la Cordillera Nordpatagónica. Rev. Asoc. Geol. Argent. 66 (3), 399–405.
Asensio, M., Zavala, C., Arcuri, M., 2004. Evidencias de la acción de mareas en la Cuenca de Ñirihuau. X Reunión Argentina de Sedimentología. Acta de resúmenes 19–21.
Asensio, M., Zavala, C., Arcuri, M., 2005. Los sedimentos terciarios del Río Foyel, provincia de Río Negro, Argentina. Actas 16° Congreso Geológico Argentino, La Plata, pp. 271–276.

Barreda, V., García, V.E., Quattrocchio, M.E., Volkheimer, W., 2003. Palynostratigraphic analysis of the río Foyel formation (latest oligocene-early Miocene), northwestern Patagonia, Argentina. Rev. Espanola Micropaleontol. 35 (2), 229–239.
Basei, M.A.S., Brito Neves, B.B., Varela, R., Texeira, W., Siga Jr., O., Sato, A.M., Cingolani, C.A., 1999. Isotopic Dating on the Crystalline Basement Rocks of the Bariloche Region, Rio Negro, Argentina. II South American Symposium on Isotope Geology, pp. 15–18.
Bates, C.C., 1953. Rational theory of delta formation. Bull. Am. Assoc. Petrol. Geol. 37, 2119–2162.
Bechis, F., 2004. Geología y estructura del sector medio de los ríos Ñirihuau y Pichi Leufú, provincia de Río Negro. Trabajo Final de Licenciatura, Universidad de Buenos Aires.
Bechis, F., Cristallini, E., 2005. Tectonic Evolution of Northern Ñirihuau Basin, Northwestern Patagonia, Argentina. Abstracts 6° International Symposium of Andean Geodinamics (ISAG), pp. 103–106. Barcelona, España.
Bechis, F., Cristallini, E., 2006. Inflexiones en estructuras del sector norte de la faja plegada y corrida de Ñirihuau, provincia de Río Negro. Revista de la Asociación Geológica Argentina, Serie D, Publicación Especial N°6, pp. 18–25.
Bechis, F., Encinas, A., Concheyro, A., Litvak, V.D., Aguirre-Urreta, B., Ramos, V.A., 2014a. New age constraints for the Cenozoic marine transgressions of north- western Patagonia, Argentina (41°- 43°S): paleogeographic and tectonic implications. J. S. Am. Earth Sci. 52, 72–93.
Bechis, F., Encinas, A., Litvak, V.D., Valencia, V., Ramos, V.A., 2014b. Nuevas edades U-Pb del relleno de la cuenca de Ñirihuau, Andes Nordpatagonicos. Actas 19° n. Congreso Geológico Argentino, Córdoba, Córdoba, pp. 15698–15699.
Bechis, F., Encinas, A., Valencia, V.A., Ramos, V.A., 2015. Analyzing the transition from extension to contraction at the north patagonian Andes. Actas 14° Congreso Geológico Chileno, La Serena, pp. 737–739.
Benedini, L., Geraldes, M., Gregori, D.A., Strazzere, L., Marcos, P., Barros, M., 2017. Nueva edad U-Pb Eocena tardía para la Formación Ventana, Andes Nordpatagónicos, Provincia de Río Negro. Actas 20° Congreso Geológico Argentino, pp. 7–11. San Miguel de Tucumán.
Bhattacharya, J.P., 2006. Deltas. In: Posamentier, H.W., Walker, R.G. (Eds.), Facies Models Revisited, vol. 84. SEPM Special Publication, pp. 237–292.
Bilmes, A., D'Elia, L., Franzese, J., Veiga, G., Hernández, M., 2013. Miocene block uplift and basin formation in the Patagonian foreland: the Gastre Basin, Argentina. Tectonophysics 601, 98–111.
Blair, T.C., McPherson, J.G., 1994a. Alluvial fans and their natural distinction from rivers based on morphology, hydraulic processes, sedimentary processes, and facies assemblages. J. Sediment. Res. 64 (3), 450–489.
Blair, T.C., McPherson, J.G., 1994b. Alluvial fan processes and forms. In: Abrahams, A. D., Parsons, A.J. (Eds.), *Geomorphology Of Desert Environments*. Springer, Dordrecht, pp. 354–402.
Bocchino, R.A., 1964. Sobre un Pygidiidae (Pisces, Siluriformes) del Eoceno de Río Negro. Ameghiniana 3 (7), 185–189.
Boggs, S., 2009. Petrology of Sedimentary Rocks, second ed. University of Oregon.
Bornhold, B.D., Prior, D.B., 1990. Morphology and sedimentary processes on the subaqueous noeick river delta, British columbia, Canada. In: Colella, A., Prior, D.B. (Eds.), Coarse-Grained Deltas. Blackwell Publishing Ltd., Oxford, UK, pp. 169–181.
Bridge, J.S., 2006. Fluvial facies models: recent developments. In: Posamentier, H.W., Walker, R.G. (Eds.), Facies Models Revisited, vol. 84. SEPM Special Publication, pp. 85–170.
Bridge, J.S., Tye, R.S., 2000. Interpreting the dimensions of ancient fluvial channel bars, channels, and channel belts from wireline-logs and cores. Bull. Am. Assoc. Pet. Geol. 84, 1205–1228.
Butler, K.L., Horton, B.K., Echaurren, A., Folguera, A., Fuentes, F., 2020. Cretaceous-Cenozoic growth of the Patagonian broken foreland basin, Argentina: chronostratigraphic framework and provenance variations during transitions in Andean subduction dynamics. J. S. Am. Earth Sci. 97, 102242.
Castro, A., Moreno- Ventas, I., Fernández, C., Vujovich, G., Gallastegui, G., Heredia, N., Martino, R.D., Becchio, R., Corretgé, L.G., Díaz-Alvarado, J., Such, P., García-Arias, M., Liu, D.Y., 2011. Petrology and SHRIMP U-Pb zircon geochronology of Cordilleran granitoids of the Bariloche area, Argentina. J. S. Am. Earth Sci. 32 (4), 508–530.
Cavazza, W., 1989. Detrital modes and provenance of the stilo-capo d'Orlando formation (Miocene), southern Italy. Sedimentology 36 (6), 1077–1090.
Caviglia, N., Zamaloa, M.D.C., 2014. Flora angiospérmica de Pico quemado, formación Ñirihuau (oligoceno tardío), provincia de Río Negro, Argentina. Ameghiniana 51 (3), 209–225.
Caviglia, N., 2018. Early Miocene climate estimations in Patagonia: the case of pico quemado, Ñirihuau Formation (Lower-Middle Miocene). J. S. Am. Earth Sci. 88, 64–71.
Cazau, L.B., 1972. Cuenca de Ñirihuau- Ñorquinco- cushamen. In: Leanza, A. (Ed.), Geología Regional Argentina. Academia Nacional de Ciencias de Córdoba, pp. 727–740.
Cazau, L.B., 1980. Cuenca de Ñirihuau- Ñorquinco- cushamen. In: Turner, J.C. (Ed.), Geología Regional Argentina. Academia Nacional de Ciencias de Córdoba, pp. 1149–1171.
Cazau, L.B., Mancini, D., Cangini, J., Spalleti, L.A., 1989. Cuenca de Ñirihuau. In: Chebli, G.A. (Ed.). In: y Spalletti, L.A. (Ed.), Cuencas Sedimentarias Argentinas, vol. 6, pp. 299–318.
Cazau, L.B., Cortiñas, J., Reinante, S., Asensio, M., Bechis, F., Apreda, D., 2005. Cuenca de Ñirihuau. In: Chebli, G.A., Cortiñas, J., Spalletti, L.A., Legarreta, L., Vallejo, E.L. (Eds.), Frontera Exploratoria de la Argentina. 6° Congreso de Exploración y Desarrollo de Hidrocarburos, pp. 251–273. Mar del Plata, Argentina.
Chang, Z., Vervoort, J.D., McClelland, W.C., Knaack, C., 2006. U-Pb dating of zircon by LA-ICP-MS. G-cubed 7 (5), Q05009.
Cione, A.L., Báez, A.M., 2007. Peces continentales y anfibios cenozoicos de Argentina los últimos cincuenta años. Asociación Paleontológica Argentina, Ameghiniana 50° Aniversario. Publicación Especial 11 (1), 195–220.
Collinson, J.D., Thompson, D.B., 1989. Sedimentary Structures: London. Chapman & Hall, p. 207.
Corner, G., Nordahl, E., Munch-Ellingsen, Robertsen, K., 1990. Morphology and sedimentology of an emergent fjord-head Gilbert-type delta: alta delta, Norway. In: Colella, A., Prior, D. (Eds.), Coarse-grained Deltas, vol. 10. International Association of Sedimentologists, pp. 155–168.
Dalla Salda, L., Franzese, J., 1987. Las megafracturas del Macizo y la Cordillera Nordpatagónica y la génesis de las cuencas volcano-sedimentarias terciarias. Rev. Geol. Chile 31, 3–13.
Davidson, W., 1993. Iron and manganese in lakes. Earth Sci. Rev. 34 (2), 119–163.
DeCelles, 2012. Foreland basin systems revisited: variations in response to tectonic settings. In: Busby, C., Azor Pérez, A. (Eds.), Tectonics of Sedimentary Basins: Recent Advances. Blackwell Publishing Ltd., pp. 405–426
Dessanti, R., 1972. Andes patagónicos septentrionales. In: Leanza, A.F. (Ed.), Geología Regional Argentina. Academia Nacional de Ciencias, Córdoba, pp. 655–687.
Dickinson, W.R., 1985. Interpreting provenance relations from detrital modes of sandstones. In: Zuffa, G.G. (Ed.), Provenance of Arenites. Reidel Publishing Company, pp. 333–361.
Dickinson, W.R., Beard, L.S., Brakenridge, G.R., Erjavec, J.L., Inman, K.F., Knepp, R.A., Lindberg, F.A., Ryberg, P.T., 1983. Provenance of North American Phanerozoic sandstones in relation to tectonic setting. Geol. Soc. Am. Bull. 94, 222–235.
Dickinson, W.R., Gehrels, G.E., 2009. Use of U–Pb ages of detrital zircons to infer maximum depositional ages of strata: a test against a Colorado Plateau Mesozoic database. Earth Planet Sci. Lett. 288 (1–2), 115–125.
Diez, O.M., Zubia, M.A., 1981. Sinopsis estratigráfica de la región de "El Bolsón", provincia de Río Negro. Revista de la Asociación Geológica Argentin a 36 (1), 19–28.
Dunham, R.J., 1962. Classification of carbonate rocks according to depositional texture. In: Ham, W.E. (Ed.), Classification of Carbonate Rocks. American Association of Petroleum Geologists, pp. 108–121.
Echaurren, A., Folguera, A., Gianni, G., Orts, D., Tassara, A., Encinas, A., Giménez, M., Valencia, V., 2016. Tectonic evolution of the North Patagonian Andes (41°–44° S) through recognition of syntectonic strata. Tectonophysics 677, 99–114.
Eilertsen, R.S., Corner, G.D., Aasheim, O., Hansen, L., . Facies characteristics and architecture related to palaeodepth of Holocene fjord–delta sediments. Sedimentology 58, 1784–1809.
Einsele, G., 1992. Sedimentary Basins: Evolution, Facies and Sediment Budget. Springer Verlag, Berlin, p. 628.
Escosteguy, L., Geuna, S.E., Franchi, M.L., Gonzalez Diaz, E.F., y Dal Molin, C., 2013. Hoja Geológica 4172-II, San Martín de los Andes, Provincias de Río Negro y Neuquén: Programa Nacional de Cartas Geológicas de la República Argentina 1: 250.000. Servicio Geológico Nacional, vol. 409. Boletín del Servicio Geológico Argentino, p. 99.
Falaschi, P., Zamaloa, M.D.C., Caviglia, N., Romero, E.J., 2012. Flora gimnospérmica de la Formación Ñirihuau (oligoceno tardío-mioceno temprano), provincia de Río Negro, Argentina. Ameghiniana 49 (4), 525–551.
Fernández Paz, L., Litvak, V.D., Echaurren, A., Ianelli, S.B., Encinas, A., Folguera, A., Valencia, V., 2018. Late Eocene volcanism in north Patagonia (42°30′–43°S): arc resumption after a stage of within-plate magmatism. J. Geodyn. 113, 13–31.
Fernández Paz, L., Bechis, F., Litvak, V.D., Echaurren, A., Encinas, A., González, J., Lucassen, F., Oliveros, V., Valencia, V., Folguera, A., 2019. Constraints on trenchward arc migration and backarc magmatism in the north patagonian Andes in the context of nazca plate rollback. Tectonics 38 (11), 3794–3817.
Fernández Paz, L., Iannelli, S.B., Echaurren, A., Ramos, M., Bechis, F., Litvak, V.D., Encinas, A., Kasemann, S., Lucassen, F., Folguera, A., 2020. The late Eocene–early Miocene El Maitén Belt evolution: magmatic response to the changing subduction zone geodynamics. J. S. Am. Earth Sci. 103, 102713.
Feruglio, E., 1941. Nota preliminar sobre la hoja geológica "San Carlos de Bariloche" (Patagonia), 200. Boletín de Informaciones Petroleras, pp. 27–64.
Feruglio, E., 1947. Hoja 40b, "San Carlos de Bariloche", Territorio Nacional de Río Negro. Mapa a escala 1:200.000. Dirección General de Minas y Geología, Buenos Aires.
Feruglio, E., 1949-1950. Descripción geológica de la Patagonia. Yacimientos petrolíferos fiscales. Ministerio Industria y Comercio 2, 336–338.
Fisher, R.V., 1961. Proposed classification of volcaniclastic sediments and rocks. Geol. Soc. Am. Bull. 72 (9), 1409–1414.
Folguera, A., Ramos, V.A., 2002. Partición de la deformación durante el Neógeno en los Andes Patagónicos Septentrionales (37°- 46°S). Rev. Soc. Geol. Espana 15 (1–2), 81–93.
Folguera, A., Orts, D., Spagnuolo, M., Rojas Vera, E., Litvak, V.D., Sagripanti, L., Ramos, M.E., Ramos, V.A., 2011. A review of late cretaceous to quaternary palaeogeography of the southern Andes. Biol. J. Linn. Soc. 103, 250–268.
Folk, R.L., Andrews, P.B., Lewis, D.W., 1970. Detrital sedimentary rock classification and nomenclature for use in New Zealand. N. Z. J. Geol. Geophys. 13, 937–968.
Forel, E.A., 1892. Le Leman: monographie Limnologique. In: Geographie, Hydrographie, Geologie, Climatologie, Hydrologie, vol. 1. E Rouge, Lausanne, p. 543.
French, P., 2007. Deltaic and estuarine environments. In: Perry, C., Taylor, K. (Eds.), Environmental Sedimentology. Blackwell Publishing, pp. 223–262.
García Morabito, E., Beltrán-Triviño, A., Terrizzano, C.M., Bechis, F., Likerman, J., Von Quadt, A., Ramos, V.A., 2021. The influence of climate on the dynamics of mountain building within the Northern Patagonian Andes. Tectonics 40 (2), e2020TC006374.

Gawthorpe, R.L., Leeder, M.R., 2000. Tectono-sedimentary evolution of active extensional basins. Basin Res. 12 (3–4), 195–218.
Giacosa, R., Heredia, N., 1999. La cuenca de antepaís terciaria asociada a la faja plegada y corrida de los Andes Patagónicos entre los 41° y 42° S, SO de Argentina. Acta Geol. Hisp. 32, 103–111.
Giacosa, R., Heredia, N., 2004a. Structure of the North Patagonian thick-skinned fold-and-thrust belt, southern central Andes, Argentina (41°-42° S). J. S. Am. Earth Sci. 18, 61–72.
Giacosa, R., Heredia, N., 2004b. Estructura de los Andes Nordpatagónicos en los cordones Piltriquitrón y Serrucho y en el valle de El Bolsón (41°30′ - 42°00′ S), Río Negro. Rev. Asoc. Geol. Argent. 59 (1), 91–102.
Giacosa, R., Heredia, N., Césari, O., Zubia, M., González, R., Faroux, A., 2001. Descripción geológica de la Hoja 4172-IV, san Carlos de Bariloche, provincias de Río Negro y neuquén. Servicio Geológico Minero Argentino, Instituto de Geología y Recursos Minerales, Boletín 279. Buenos Aires.
Giacosa, R.E., Alfonso, J.C., Heredia, N., Paredes, J., 2005. Tertiary tectonics of the sub-Andean region of the North Patagonian Andes, southern central Andes of Argentina (41-42°30′S). J. S. Am. Earth Sci. 20, 157–170.
Gianni, G., Navarrete, C., Liendo, I., Diaz, M., Giménez, M., Encinas, A., Folguera, A., 2018. Cretaceous intraplate contraction in southern Patagonia: a far-field response to changing subduction dynamics? Tectonics 37, 2915.
Glenn, C.R., Kelts, K., 1991. Sedimentary rhythms in lake deposits. In: Einsele, G., Ricken, W., Seilacher, A. (Eds.), Cycles and Events in Stratigraphy, pp. 188–221.
González, P., Coluccia, A., Franchi, M., 2000. Hoja Geológica 4169-III Ingeniero Jacobacci. Provincia de Río Negro. Programa Nacional de Cartas Geológicas de la República Argentina 1:250.000, vol. 311. Servicio Geológico Minero Argentino, Boletín, Buenos Aires.
González Bonorino, F., 1944. Descripción geológica y petrográfica de la Hoja geológica 41b río Foyel (río Negro), 56. Dirección Nacional Minería e Hidrogeología, p. 124.
González Bonorino, F., 1973. Geología del área entre San Carlos de Bariloche y Llao-Llao. Fundación Bariloche, Publicación 16, 1–53.
González Bonorino, F., González Bonorino, G., 1978. Geología de la región de San Carlos de Bariloche: un estudio de las formaciones terciarias del Grupo Nahuel Huapi. Rev. Asoc. Geol. Argent. 33 (3), 175–210.
González Díaz, E.F., 1979. La edad de la Formación Ventana en el área al norte y al este del lago Nahuel Huapi. Rev. Asoc. Geol. Argent. 34 (2), 113–124.
González Díaz, E.F., 1982. Zonación cronológica del plutonismo en los Andes Patagónicos Septentrionales entre los 40 y 42 sur: la migración de los ciclos intrusivos. Acta Geol. Lilloana 16 (1), 5–22.
González Díaz, E., Nullo, F., 1980. Cordillera neuquina. In: Leanza, A. (Ed.), Geología Regional Argentina, vol. 2. Academia Nacional de Ciencias, Córdoba, pp. 1099–1147.
Gordon, A., Ort, M., 1993. Edad y correlación del plutonismo subcordillerano en las provincias de Río Negro y Chubut, vol. 4. Actas 12° Congreso Geológico Argentino, Buenos Aires, pp. 120–127.
Groeber, P., 1954. La Serie Andesítica Paleógena, sus relaciones, posición y edad. Rev. Asoc. Geol. Argent. 9 (2), 39–42.
Hampton, B.A., Horton, B.K., 2007. Sheetflow fluvial processes in a rapidly subsiding basin, Altiplano plateau, Bolivia. Sedimentology 54 (5), 1121–1148.
Harms, J.C., Southard, J.B., Walker, R.G., 1982. Structures and sequences in clastic rocks. In: SEPM Short Course, vol. 9, p. 51. Lecture Notes. Society of Economic Paleontologists and Mineralogists, Calgary.
Hervé, F., Calderón, M., Fanning, M.C., Pankhurst, R.J., Rapela, C.W., Quezada, P., 2018. The country rocks of devonian magmatism in the north patagonian massif and chaitenia. Andean Geol. 45 (3), 301–317.
Hogg, S.E., 1982. Sheefloods, sheetwash, sheetflow or…? Earth Sci. Rev. 18 (1), 59–76.
Horton, B.K., 2018. Tectonic regimes of the central and southern Andes: responses to variations in plate coupling during subduction. Tectonics 37 (2), 402–429.
Iannelli, S.B., Litvak, V.D., Fernandez Paz, L., Folguera, A., Ramos, M.E., Ramos, V.A., 2017. Evolution of Eocene to Oligocene arc-related volcanism in the north patagonian Andes (39–41°S), prior to the break-up of the farallon plate. Tectonophysics 696–697, 70–87.
Iannelli, S., Fernández Paz, L., Litvak, V.D., Gianni, G.M., Fennell, L.M., González, J., Lucassen, F., Kasemann, S., Oliveros, V., Folguera Telichevsky, A., 2020. Southward-directed subduction of the farallon–aluk spreading ridge and its impact on subduction mechanics and andean arc magmatism: insights from geochemical and seismic tomographic data. Front. Earth Sci. 8, 121.
Ingersoll, R.V., Bullard, T.F., Ford, R.L., Grimm, J.P., Pickle, J.D., Sares, S.W., 1984. The effect of grain size on detrital modes: a test of the Gazzi-Dickinson point-counting method. J. Sediment. Res. 54 (1), 103–116.
Jordan, T.E., Matthew Burns, W., Veiga, R., Pangaro, F., Copeland, P., Kelley, S., Mpodozis, C., 2001. Extension and basin formation in the Southern Andes caused by increased convergence rate: a mid-Cenozoic trigger for the Andes. Tectonics 20 (3), 308–324.
Lambert, A.M., Kelts, K.R., Marshall, N.E., 1976. Measurements of density underflows from Walensee, Switzerland. Sedimentology 23, 87–105.
Lara, L.E., Rodriguez, C., Moreno, H., Pérez de Arce, C., 2001. Geocronología K- Ar y geoquímica de volcanismo plioceno superior- pleistoceno de los Andes del Sur (398-42 8S). Rev. Geol. Chile 28 (1), 67–90.
Lavenu, A., Cembrano, J., 1999. Compressional- and transpressional-stress pattern for Pliocene and Quaternary brittle deformation in fore arc and intra-arc zones (Andes of Central and Southern Chile). J. Struct. Geol. 21, 1669–1691.
Link, M.H., Osborne, R.H., Awramik, S.M., 1978. Lacustrine stromatolites and associated sediments of the Pliocene ridge route formation, ridge basin, California. J. Sediment. Res. 48 (1), 143–157.
Ljungner, E., 1931. Geologische aufnahmen in der Patagonischen kordillera. Bulletin Geological Institut Uppsala 23, 203–242.
Ludwig, K.R., 2003. Isoplot 3.0—A Geochronological Toolkit for Microsoft Excel: Special Publication No. 4. Berkeley Geochronology Center, Berkeley, Calif., p. 71
Makaske, B., 2001. Anastomosing rivers: a review of their classification, origin and sedimentary products. Earth Sci. Rev. 53 (3–4), 149–196.
Mancini, D., Serna, M., 1989. Evaluación petrolera de la Cuenca de Ñirihuau. Sudoeste de Argentina. Actas 1° Congreso Nacional de Exploración de Hidrocarburos, Buenos Aires, Argentina, pp. 739–762.
Marrett, R.A., Allmendinger, R.W., 1990. Kinematic analysis of fault-slip data. J. Struct. Geol. 12, 973–986.
McPhie, J., Doyle, M., Allen, R., Allen, R.L., 1993. Volcanic Textures: A Guide to the Interpretation of Textures in Volcanic Rocks. Centre for Ore Deposit and Explorations Studies, University of Tasmania, p. 211.
Miall, A.D., 1978. Lithofacies types and vertical profile models of braided river deposits, a summary. In: Miall, A.D. (Ed.), Fluvial Sedimentology, vol. 5. Memoir Canadian Society Petrology Geology, Calgary, pp. 597–604.
Miall, A.D., 1985. Architectural-element analysis: a new method of facies analysis applied to fluvial deposits. Earth Sci. Rev. 22 (4), 261–308.
Miall, A.D., 1996. The geology of fluvial deposits. Sedimentary Facies, Basin Analysis, and Petroleum Geology. Springer-Verlag, New York, p. 582.
Munizaga, F., Hervé, F., Drake, R., Pankhurst, R.J., Brook, M., Snelling, N., 1988. Geochronology of the lake region of south-central Chile (39–42 S): preliminary results. J. S. Am. Earth Sci. 1 (3), 309–316.
Nemec, W., 1990. Aspects of sediment movement on steep delta slopes. In: Colella, A., Prior, D. (Eds.), Coarse-grained Deltas. International Association of Sedimentologists, pp. 29–73.
Nichols, G., 2009. Sedimentology and Stratigraphy. John Wiley & Sons.
Oriolo, S., Schulz, B., González, P.D., Bechis, F., Olaizola, E., Krause, J., Renda, E.M., Vizán, H., 2019. The late paleozoic tectonometamorphic evolution of Patagonia revisited: insights from the pressure-temperature-deformation-time (P-T-D-t) path of the gondwanide basement of the north patagonian cordillera (Argentina). Tectonics 38 (7), 2378–2400.
Orts, D., Folguera, A., Encinas, A., Ramos, M., Tobal, J., Ramos, V., 2012. Tectonic development of the North Patagonian Andes and their related Miocene foreland basin (41°30'- 43°S). Tectonics 31 (3), 24.
Orts, D., Folguera, A., Gimenez, M., Ruiz, F., Rojas Vera, E., Lince Klinger, F., 2015. Cenozoic building and deformational processes in the north patagonian Andes. J. Geodyn. 86, 26–41.
Pankhurst, R.J., Rapela, C.W., Fanning, C.M., Márquez, M., 2006. Gondwanide continental collision and the origin of Patagonia. Earth Sci. Rev. 76, 235–257.
Pardo-Casas, F., Molnar, P., 1987. Relative motion of the nazca (farallón) and south American plates since late cretaceous time. Tectonics 6, 233–248.
Paredes, J.M., Giacosa, R.E., Heredia, N., 2009. Sedimentary evolution of neogene continental deposits (Ñirihuau Formation) along the Ñirihuau river, North Patagonian Andes of Argentina. J. S. Am. Earth Sci. 28, 74–88.
Pascual, R., Bondesio, P., Vucetich, M., Scillato Yané, G., Bond, M., Tonni, E., 1984. Vertebrados fósiles cenozoicos. In: Ramos, V. (Ed.), Geología y Recursos Naturales de la Provincia de Río Negro. Buenos Aires, vol. 2, pp. 439–461, 9.
Passalia, M.G., Bechis, F., 2012. Megafloras de la sección basal de la Formación Ñirihuau (Oligoceno Superior?- Mioceno Inferior) en las localidades Pico Quemado y Cordón de las Bayas, provincia de Río Negro, Argentina. 15° Simposio Argentino de Paleobotánica y Palinología. Corrientes, Resúmenes en CD-ROM.
Passalia, M., Cavigglia, N., Vera, E., 2019. Lithraea australis (Berry) comb. nov. (Anacardiaceae) from the upper section of Ñirihuau Formation (middle Miocene), Patagonia. Rev. Palaeobot. Palynol. 266, 1–11.
Pettijohn, F.J., Potter, P.E., Siever, R., 1973. Sand and Sandstone. Springer-Verlag, New York, p. 618p.
Pharo, C.H., Carmack, E.C., 1979. Sedimentation processes in a short residence time intermontane lake, Kamloops Lake, British Columbia. Sedimentology 26, 523–541.
Posamentier, H.W., Walker, R.G., 2006. Facies Models Revisited. SEPM. Special Publication, p. 84.
Powers, M., 1953. A new roundness scale for sedimentary particles. J. Sediment. Res. 23, 117–119.
Rabassa, J., 1978. Estratigrafía de la región de Pilcaniyeu- Comallo, Provincia de Río Negro. Actas 7° Congreso Geológico Argentino, Buenos Aires, pp. 731–746.
Ramos, M.E., Orts, D., Calatayud, F., Folguera, A., Ramos, V., 2011. Reevaluación de la génesis de la Cuenca de Ñirihuau a la altura del Cordón del Maitén, Faja Plegada de Cushamen, Provincia de Chubut. Actas 18° Congreso Geológico Argentino, Neuquén. Published on-line.
Ramos, M.E., Orts, D.L., Calatayud, F., Pazos, P.J., Folguera, A., Ramos, V.A., 2011. Estructura, Estratigrafía y evolución tectónica de la cuenca de Ñirihuau en las nacientes del río Cushamen, Chubut. Rev. Asoc. Geol. Argent. 68, 210–224.
Ramos, M.E., Tobal, J.E., Sagripanti, L., Folguera, A., Orts, D.L., Giménez, M., Ramos, V. A., 2015. The North Patagonian orogenic front and related foreland evolution during the Miocene, analyzed from synorogenic sedimentation and U/Pb dating (~ 42° S). J. S. Am. Earth Sci. 64, 467–485.
Ramos, V.A., 1982. Las ingresiones pacíficas del Terciario en el norte de la Patagonia (Argentina). 3° Congreso Geológico Chileno 262–288.
Ramos, V.A., 1988. Tectonics of late proterozoic-early paleozoic: a collisional history of southern south America. Episodes 11 (3), 168–174.
Ramos, V.A., 1999. Las Provincias Geológicas del Territorio Argentino. In: Caminos, R. (Ed.), Geología Argentina, vol. 29. Instituto de Geología y Recursos Minerales, Buenos Aires, Anales, pp. 41–96, 3.

Ramos, V.A., Cortés, J.M., 1984. Estructura e interpretación tectónica. In: Ramos, V.A. (Ed.), Geología y Recursos Naturales de la Provincia de Río Negro, vol. 1. Actas 9° Congreso Geológico Argentino, pp. 317–346, 12.
Ramos, V.A., Ghiglione, M.C., 2008. Tectonic evolution of the patagonian Andes. Dev. Quat. Sci. 11, 57–71.
Rapela, C.W., Spalletti, L.A., Merodio, J.C., Aragón, E., 1988. Temporal evolution and spatial variation of early Tertiary volcanism in the Patagonian Andes (40°S - 42°30'S). J. S. Am. Earth Sci. 1, 75–88.
Ravazzoli, I., Sesana, F., 1977. Descripción geológica de la Hoja 41c Río Chico. Servicio Geológico Nacional. Boletín, Buenos Aires, p. 148.
Reading, H.G., 1996. Sedimentary Environments: Processes, Facies and Stratigraphy, third ed. Blackwell Science, Cambridge, Mass.
Reading, H.G., Collinson, J.D., 1996. Clastic coasts. In: Reading, H.G. (Ed.), Sedimentary Environments: Processes, Facies and Stratigraphy, third ed. Blackwell Science, Cambridge, Mass, pp. 154–231.
Rosenau, M., Melinck, D., Echtler, H., 2006. Kinematic constraints on intra-arc shear and strain partitioning in the southern Andes between 38°S and 42°S latitude. Tectonics 25, TC4013.
Roth, S., 1922. Investigaciones geológicas en la región norte de la Patagonia durante los años 1897 y 1898, vol. 26. Revista Museo de la Plata, pp. 393–473.
SERNAGEOMIN, 2003. Mapa Geológico de Chile, Versión Digital, Base Geológica escala 1:1.000.000. Publicación Geológica Digital, No. 4, CD-ROM, versión 1.0. Servicio Nacional de Geología y Minería.
Sharman, G.R., Malkowski, M.A., 2020. Needles in a haystack: detrital zircon UPb ages and the maximum depositional age of modern global sediment. Earth Sci. Rev. 203, 103109.
Smith, D.G., 1986. Anastomosing river deposits, sedimentation rates and basin subsidence, Magdalena River, northwestern Colombia, South America. Sediment. Geol. 46 (3–4), 177–196.
Smith, D.G., Smith, N.D., 1980. Sedimentation in anastomosed river systems; examples from alluvial valleys near Banff, Alberta. J. Sediment. Res. 50 (1), 157–164.
Smith, G.A., 1991. Facies sequences and geometries in continental volcaniclastic sediments. In: Fisher, R.V., Smith, G.A. (Eds.), Sedimentation in Volcanic Settings, pp. 109–120.
Smith, N.D., Cross, T.A., Dufficy, J.P., Clough, R.S., 1989. Anatomy of an avulsion. Sedimentology 36, 1–23.
Somoza, R., 1998. Updated Nazca (Farallon)-South America relative motions during the last 40 My: implications for mountain building in the central Andean region. J. S. Am. Earth Sci. 11 (3), 211–215.
Somoza, R., Zaffarana, C., 2008. Mid-Cretaceous polar standstill of South America, motion of the Atlantic hotspots and the birth of the Andean cordillera. Earth Planet Sci. Lett. 271 (1–4), 267–277.
Spalletti, L.A., 1981. Facies sedimentarias de la Formación Ñirihuau en la región de San Carlos de Bariloche, provincia de Río Negro. Rev. Asoc. Geol. Argent. 36 (3), 288–311.
Spalletti, L.A., 1983. Paleogeografía de la Formación Ñirihuau y sus equivalentes en la región Occidental de Neuquén, Río Negro y Chubut. Rev. Asoc. Geol. Argent. 38 (3–4), 454–468.
Spalletti, L., Dalla Salda, L., 1996. A pull apart volcanic related Tertiary Basin, an example from the Patagonian Andes. J. S. Am. Earth Sci. 9 (3–4), 197–206.
Spalletti, L.A., Merodio, J.C., De Posadas, V.G., 1982. Caracteres petrográficos y geoquímicos de las piroclastitas de la Formación Ñirihuau. Rev. Asoc. Geol. Argent. 37 (1), 50–65.
Spalletti, L.A., Matheos, S., 1987. Composición de sedimentitas silicoclásticas terciarias de la cuenca de Ñirihuau (Patagonia Occidental) y su significado tectónico. Rev. Asoc. Geol. Argent. 42 (3–4), 322–337.
Stern, C.R., 2004. Active Andean volcanism: its geologic and tectonic setting. Rev. Geol. Chile 31 (2), 161–206.
Talbot, M.R., Allen, P.A., 1996. Lakes. In: Reading, H.G. (Ed.), Sedimentary Environments: Processes, Facies and Stratigraphy, third ed. Blackwell Science, Cambridge, Mass, pp. 83–124.
Taylor, J.M., 1950. Pore-space reduction in sandstones. Bull. Am. Assoc. Pet. Geol. 34 (4), 701–716.
Thomson, S.N., 2002. Late Cenozoic geomorphic and tectonic evolution of Patagonian Andes between latitudes 42°S and 46°S: an appraisal based on fission-track results from the transpressional intra-arc Liquiñe-Ofqui fault zone. Geol. Soc. Am. Bull. 114 (9), 1159–1173.
Tobal, J.E., Rojas Vera, E., Folguera, A., Ramos, V.A., 2012. Deformación andina en el cordón del Hielo Azul al oeste de El Bolsón: implicancias en la evolución tectónica de la Cordillera Norpatagónica en Río Negro, Argentina. Andean Geol. 39 (3), 442–463.
Tobal, J.E., Folguera, A., Likerman, J., Naipauer, M., Sellés, D., Boedo, F.L., Ramos, V.A., Gimenez, M., 2015. Middle to late Miocene extensional collapse of the north patagonian Andes (41° 30′–42° S). Tectonophysics 657, 155–171.
Toubes, R., Spikerman, J., 1973. Algunas edades K/Ar y Rb/Sr de las plutonitas de la Cordillera Patagónica entre los paralelos 40-44 de latitud sur. Rev. Asoc. Geol. Argent. 28 (4), 382–439.
Tucker, M.E., 2009. Sedimentary Petrology: an Introduction to the Origin of Sedimentary Rocks. Blackwell Science.
Tunbridge, I.P., 1981. Sandy high-energy flood sedimentation – some criteria for recognition, with an example from the Devonian of SW England. Sediment. Geol. 28, 79–95.
Varela, R., Basei, M., Brito Neves, B., Sato, A., Teixeira, W., Cingolani, C., Siga Jr., O., 1999. Isotopic Study of Igneous and Metamorphic Rocks of Comallo-Paso Flores, Río Negro, Argentina. II South American Symposium on Isotope Geology, pp. 148–151.
Varela, R., Basei, M.A., Cingolani, C.A., Siga Jr., O., Passarelli, C.R., 2005. El basamento cristalino de los Andes Norpatagónicos en Argentina: geocronología e interpretación tectónica. Rev. Geol. Chile 32 (2), 167–187.
Volkheimer, W., 1964. Estratigrafía de la zona extrandina del Departamento de Cushamen (Chubut) entre los paralelos 42° y 42°30′ y los meridianos 70° y 71°. Rev. Asoc. Geol. Argent. 19 (2), 85–107.
Weirich, E.H., 1986. A study of the nature and incidence of density currents in a shallow glacial lake. Ann. Assoc. Am. Geogr. 76, 396–413.
Wentworth, C.K., 1922. A scale of grade and class terms for clastic sediments. J. Geol. 30 (5), 377–392.
White, J.D.L., Houghton, B.F., 2006. Primary volcaniclastic rocks. Geology 34 (8), 677–680.
Williams, G.E., 1971. Flood deposits of the sandbed ephemeral streams of central Australia. Sedimentology 17, 1–40.
Wright, V.P., 1992. A revised classification of limestones. Sediment. Geol. 76, 177–185.